PCIF1 catalyzes m6Am mRNA methylation to regulate gene expression

Erdem Sendinc[1,2,3], David Valle-Garcia[1,2,3], Abhinav Dhall[1,2], Hao Chen[1,2], Telmo Henriques[3], Wanqiang Sheng[1,2], Karen Adelman[3], Yang Shi[1,2,*]

[3] These authors contributed equally to this work

Affiliations

1 Division of Newborn Medicine and Epigenetics Program, Department of Medicine, Boston Children's Hospital, Boston, Massachusetts 02115, USA.

2 Department of Cell Biology, Harvard Medical School, Boston, Massachusetts 02115, USA.

3 Department of Biological Chemistry and Molecular Pharmacology, Harvard Medical School, Boston, Massachusetts 02115, USA.

* Correspondence: yang_shi@hms.harvard.edu (Y.S.)

Highlights

- PCIF1 is an evolutionarily conserved mRNA m6Am methyltransferase
- Loss of PCIF1 leads to a complete loss of m6Am, whereas m6A level and distribution are not affected
- PCIF1 mediated m6Am does not affect RNA Pol II transcription or mRNA stability
- m6Am-Exo-Seq is a robust methodology that enables global m6Am mapping
- m6Am suppresses cap dependent translation

Summary

mRNA modifications play an important role in regulating gene expression. One of the most abundant mRNA modifications is N6,2-O-dimethyladenosine (m6Am). Here, we demonstrate that m6Am is an evolutionarily conserved mRNA modification mediated by the Phosphorylated CTD Interacting Factor 1 (PCIF1), which catalyzes m6A methylation on 2-O-methylated adenine located at the 5' ends of mRNAs. Furthermore, PCIF1 catalyzes only 5' m6Am methylation of capped mRNAs, but not internal m6A methylation *in vitro* and *in vivo*. Our global mRNA methylation analysis revealed that there is no crosstalk between m6Am and m6A mRNA methylation events, suggesting that m6Am is functionally distinct from m6A. Importantly, our data indicate that m6Am negatively impacts translation of methylated mRNAs by antagonizing cap binding protein eIF4E. Together, we identify the first and only human mRNA m6Am methyltransferase and demonstrate a novel mechanism of gene expression regulation through PCIF1-mediated m6Am mRNA methylation in eukaryotes.

Keywords:

mRNA modifications, m6Am, PCIF1, translational regulation, transcriptional regulation, epitranscriptomics, cap-dependent translation, eIF4E, gene expression, m6Am-Exo-Seq

50 **Introduction**

51 An important step in the regulation of gene expression is accomplished through
52 chemical modifications of mRNAs. One of the best studied internal mRNA modifications
53 is N6-methyladenosine (m6A), which is present on a diverse set of mRNAs, typically
54 clustered around stop codons (Dominissini et al., 2012; Meyer et al., 2012). m6A is
55 catalyzed by METTL3/METTL14 complex, and this modification regulates gene
56 expression by influencing localization, stability, splicing or translation of mRNAs (Yang
57 et al., 2018). Another abundant mRNA modification is N6,2-O-dimethyladenosine
58 (m6Am), which occurs near the mRNA cap (Wei et al., 1975). 5' ends of eukaryotic
59 mRNAs typically carry a 7-methylguanosine (m7G) cap linked to the rest of the mRNA
60 by a triphosphate linkage. The first nucleotide after the m7G cap can be methylated on
61 the ribose sugar. If this first nucleotide is 2-O-methyladeonisine (Am), it can be further
62 methylated at its N6 position to generate m6Am. While the methylase mediating Am
63 methylation is known, the methyltransferase responsible for generating m6Am has not
64 been identified (Keith et al., 1978; Mauer et al., 2017). As a consequence, the impact of
65 m6Am on gene regulation is still largely unexplored.

66

67 Using multiple approaches, we provide both *in vitro* and *in vivo* evidence supporting
68 Phosphorylated CTD Interacting Factor 1 (PCIF1) as the one and only mammalian
69 m6Am methyltransferase. In order to investigate the distribution of m6Am, we
70 developed a novel transcription-wide mapping technique we name m6Am-Exo-Seq.
71 PRO-Seq, RNA-seq and m6Am-Exo-Seq analyses carried out in wildtype and PCIF1

null cells show that mRNA stability of m6Am-enriched genes is largely unaffected by the loss of PCIF1. In contrast, reporter assays carried out in PCIF1 null cells using mRNA transcripts with and without m6Am suggest that m6Am may function to suppress protein translation. Taken together, our findings identify a novel enzyme that mediates m6Am methylation in the nucleus, which impacts translation in the cytoplasm.

78 **Results**

79 **m6Am is an evolutionarily conserved RNA modification**

80 To study the biological significance of m6Am, we developed a highly sensitive mass
81 spectrometry approach (LC-MS/MS) to detect and quantify m6Am (Figure S1). The
82 triphosphate bond between the m7G cap and the first nucleotide of the mRNA is not
83 cleaved by the enzymes typically used to generate single nucleosides for LC-MS/MS
84 analysis. Therefore, without the removal of the m7G cap, only the internal m6A and Am
85 modifications are detectable in human mRNA (Figure 1B). On the other hand, m6Am is
86 detectable only after treatment with a de-capping enzyme, indicating that m6Am is
87 restricted to the first nucleotide adjacent to the m7G cap of the mRNA (Figure 1B)
88 (Linder et al., 2015). Using this protocol, we analyzed mRNA isolated from various
89 model organisms by LC-MS/MS. While m6Am was not detected in fission yeast,
90 nematode or Drosophila samples, mRNA isolated from zebrafish, mouse and human
91 cells yielded m6Am, indicating that m6Am is an evolutionary conserved mRNA
92 methylation (Figure 1C).

93

94 **PCIF1 is required for mRNA m6Am methylation *in vivo***

95 A putative methyltransferase enzyme that is conserved in zebrafish, mouse and human,
96 but absent in yeast and nematodes, is PCIF1 (Phosphorylated CTD Interacting Factor
97 1) (Figure S2) (Iyer et al., 2016). PCIF1 contains a N-terminal WW domain, which is
98 believed to mediate interactions with RNA Polymerase II (Pol II) phospho-CTD, and also
99 a putative C-terminal methyltransferase domain (Ebmeier et al., 2017; Fan et al., 2003).

100 To determine whether PCIF1 is a m6Am methyltransferase, we generated several
101 independent PCIF1 knockout (KO) clonal cell lines in human melanoma MEL624 cells
102 and determined its mRNA m6Am level by LC-MS/MS (Fig. 2A and 2B). mRNA isolated
103 from a control MEL264 cell line yielded around 0.04% m6Am/A ratio. Strikingly,
104 knocking out PCIF1 resulted in a complete loss of this modification in mRNA samples
105 (Figure 2B). We further verified the absence of m6Am in PCIF1 KO cells by performing
106 thin layer chromatography (TLC) (Figures 2C and S3A). Although PCIF1 KO resulted in
107 a complete loss of m6Am, global m6A levels did not change, suggesting that PCIF1 is
108 not required for m6A modification and that m6A is not dependent on m6Am levels
109 (Figure S3B).
110
111 To determine whether it is the intrinsic enzymatic activity of PCIF1 that is responsible for
112 m6Am methylation, we carried out rescue experiments by introducing either wild-type
113 (WT) or catalytically inactive PCIF1 (APPA) back into the KO cells. While the expression
114 of wild-type PCIF1 restored the global m6Am level in the KO cells, expression of the
115 catalytic mutant with the conserved methyltransferase NPPF motif altered to APPA did
116 not result in m6Am detectable by mass spectrometry or TLC (Figures 2C and 2D).
117 PCIF1 contains a nuclear localization signal and has been suggested to be a nuclear
118 protein (Ebmeier et al., 2017; Fan et al., 2003; Hirose et al., 2008). Consistently, we
119 confirmed that PCIF1 is predominantly nuclear localized in both rescue cell lines by
120 immunofluorescence (Figure S3C). These results indicate that PCIF1 is required for
121 mRNA m6Am modification, which likely takes place in the nucleus *in vivo*.

122 **Recombinant PCIF1 methylates capped mRNA *in vitro***

123 To determine whether this putative methyltransferase can directly catalyze m6Am, we
124 purified full length recombinant PCIF1 from bacteria (Figure S4A) and performed *in vitro*
125 methylation assays employing firefly luciferase mRNA with m7G-Am 5' cap as a
126 substrate. Wild-type recombinant enzyme generated m6Am efficiently, whereas the
127 APPA catalytic mutant did not show any activity (Figures 3A and S4B). Furthermore,
128 PCIF1 did not generate m6A or Am modifications. On the other hand, generation of
129 m6Am was accompanied by a decrease in the Am level, indicating that PCIF1 catalyzed
130 conversion of Am to m6Am (Figure 3A). Consistent with previous findings (Kruse et al.,
131 2011; Mauer et al., 2017), we failed to detect cap-adjacent m6A by TLC and PCIF1 KO
132 cells show a greater accumulation of cap-adjacent Am (Figure S3A). These *in vitro* and
133 *in vivo* data collectively suggest that PCIF1 specifically methylates Am-marked mRNAs.
134

135 We next investigated whether the m7G cap structure is required for the catalytic activity
136 of PCIF1, using de-capped luciferase mRNA with 5' Am in *in vitro* methylation assays.
137 The Am residue next to the intact m7G cap was readily converted to m6Am by
138 recombinant PCIF1. In contrast, the Am residue on de-capped mRNA was not
139 converted to m6Am, indicating that m7G cap is required for PCIF1 catalytic activity
140 (Figure 3B). To determine whether there is a size requirement for capped mRNA to
141 serve as a substrate, we used a capped RNA dinucleotide (m7G-AmG) in *in vitro*
142 methylation assays. PCIF1 efficiently generated m6Am with the dinucleotide as a
143 substrate with a K_m of 208 nM and K_{cat} at 0.34 min^{-1} (Figure 3C). This indicates that

144 capped transcripts as short as 2 nucleotides can be efficiently methylated by PCIF1
145 (Figure 3D). Given that recombinant PCIF1 efficiently methylates capped mRNAs *in*
146 *vitro* and that deletion of PCIF1 results in a complete loss of mRNA m6Am methylation
147 *in vivo*, we conclude that PCIF1 is the only mRNA m6Am methyltransferase in human
148 cells.
149

150 **Loss of PCIF1 does not affect global mRNA m6A distribution *in vivo***

151 In order to identify the mRNAs that carry m6A and m6Am, we performed MeRIP-Seq
152 with an antibody against m6A in control and PCIF1 KO cell lines. Given that m6A and
153 m6Am are structurally similar, antibodies against m6A are expected to enrich for m6Am
154 at the 5' end of the mRNAs, as has been previously suggested (Linder et al., 2015).
155 However, although we were able to identify internal m6A loci enriched around stop
156 codons, as reported previously for other cell lines (Dominissini et al., 2012; Meyer et al.,
157 2012), we observed a very modest enrichment at the 5' end of mRNAs that was mostly
158 maintained in the PCIF1 KO cells (Figures 4 and 5A). Therefore, it appears that the
159 regular m6A MeRIP-Seq protocol does not efficiently capture m6Am-enriched
160 transcripts. In agreement with our *in vitro* and *in vivo* results (Figures 3A and S3B),
161 global m6A distribution did not change in two independent PCIF1 KO lines, compared to
162 control cells (Figure 4). Deletion of PCIF1, and hence complete loss of m6Am, altered
163 neither global m6A level (Figure S3B) nor genome-wide m6A distribution (Figure 4A),
164 suggesting that m6A and m6Am are independent mRNA modifications.

165 **Development of m6Am-Exo-Seq as a robust methodology that enables**
166 **global m6Am mapping**
167 To be able to map m6Am modification transcriptome-wide, we developed a novel
168 exonuclease assisted high-throughput sequencing methodology that we call m6Am-
169 Exo-Seq (Figure S5). We performed m6Am-Exo-Seq on mRNA from control and PCIF1
170 KO cells using 8 different m6A antibodies. Our new technique allowed us to observe a
171 clear enrichment of 5' ends immediate to transcription start sites only in mRNAs from
172 control cells, but not in mRNAs from PCIF1 KO cells, suggesting that m6Am-Exo-Seq
173 specifically pull-down m6Am-enriched transcripts (Figure 5A). Seven out of the eight
174 m6A antibodies tested with m6Am-Exo-Seq resulted in a significant enrichment of
175 m6Am only in control mRNA, demonstrating the robustness of this novel methodology
176 (Figure S5).
177
178 To globally map m6Am, we applied m6Am-Exo-Seq with a monoclonal m6A antibody in
179 MEL624 cell line using three biological replicates of control and PCIF1 KO cells (Figure
180 5). We identified 640 genes that are enriched for this modification (Table S1). These
181 transcripts are among the highly expressed genes in MEL624 cell line (Figure 5B), and
182 are in diverse pathways including splicing, vesicular transport and mitochondrial
183 metabolism (Figures 5B and 5C). m6Am was also mapped in HEK293T cells previously
184 (Linder et al., 2015). While most of the m6Am transcripts are methylated in both
185 HEK293T and MEL624 cells, around 40% of m6Am transcripts are unique to MEL624

186 cells (Figure S6A), suggesting that m6Am is a dynamic epitranscriptomic mark with cell-
187 type specific patterns.
188
189 **PCIF1-mediated deposition of m6Am does not alter transcription or**
190 **stability of target genes.**
191 PCIF1 interacts with the phosphorylated C-terminal domain (CTD) of Pol II, and has
192 been implicated in negative regulation of gene expression (Ebmeier et al., 2017; Fan et
193 al., 2003; Hirose et al., 2008). However, recent studies suggest that deposition of m6Am
194 stabilizes mRNA or stimulates translation (Mauer et al., 2017), both of which would
195 increase the expression of target genes. On the other hand, a separate study failed to
196 find a correlation between m6Am methylation and mRNA stability (Wei et al., 2018). We
197 thus wished to investigate the mechanism of m6Am activity in our system, where we
198 can precisely abolish m6Am by PCIF1 KO, without perturbing m6A levels. We first
199 performed RNA-Seq in PCIF1 KO MEL624 cells and a control cell line. We defined 236
200 mRNA species that were significantly more abundant in both PCIF1 KO cell lines, and
201 304 mRNAs with reduced abundance (Figure 6A, Tables S2 and S3). To distinguish
202 whether these changes in mRNA levels were due to altered transcription mediated by
203 m6Am, we next performed PRO-Seq in control and PCIF1 KO cells. PRO-Seq
204 specifically measures engaged Pol II across the genome, providing definitive
205 information on levels of active transcription (Kwak et al., 2013). These assays were
206 spike normalized to enable accurate quantification and comparisons between samples.
207 PRO-Seq signals across the 236 up-regulated genes from RNA-seq revealed that these

208 genes were more highly transcribed in PCIF1 KO cells (Figure 6B). Likewise, down-
209 regulated genes were less actively transcribed (Figure 6B). Importantly, there was a
210 strong correlation between the changes observed in RNA-Seq and PRO-Seq, indicating
211 that changes in RNA abundance could be explained fully by altered transcription
212 (r=0.67, Figure 6D).
213
214 Furthermore, we noted no significant overlap between m6Am-enriched genes and
215 genes with significantly altered signals in RNA-Seq or PRO-Seq assays (Figure 6A,
216 Tables S1-S5). PCIF1 KO did not change RNA-seq or PRO-Seq signal within m6Am-
217 enriched genes as compared to controls (Figure 6C). Moreover, the loss of PCIF1 did
218 not alter Pol II levels or distribution at noncoding snRNA genes that are marked by
219 m6Am (Figure S6B) (Mauer et al., 2018; Wei et al., 2018). Taken together, our data
220 suggest that although PCIF1 has been reported to bind RNA Pol II, it does not play a
221 significant role in transcription at m6Am target genes. Moreover, steady-state transcript
222 levels of m6Am-marked genes, as determined by RNA-Seq in PCIF1 KO cells, are not
223 affected by the loss of this modification, suggesting that stability of m6Am-marked
224 mRNAs is not significantly affected by PCIF1-mediated methylation.
225
226 **m6Am suppresses cap-dependent translation**
227 Regulation of cap binding protein eIF4E during translation initiation is a key event in
228 protein translation control. eIF4E binds m7G cap of mRNAs and recruits other
229 translation initiation factors and ribosomes for translation initiation (Sonenberg and

230 Gingras, 1998). The C terminal loop of cap bound eIF4E is in close proximity to the first
231 nucleotide of the mRNA (Tomoo et al., 2002, 2005). The N6 residue of the cap-adjacent
232 adenine of mRNA forms a critical hydrogen bond with threonine 205 residue of human
233 eIF4E (Figure S7) (Tomoo et al., 2002, 2005). We thus hypothesized that modification
234 of this adenine by PCIF1 to form m6Am may affect this interaction and hence impact
235 translation at the initiation step. To test this, we used well established reporter assays to
236 analyze the effect of m6Am on translation efficiency. We first transfected PCIF1 KO
237 cells with EGFP mRNA with either m7G-Am or m7G-m6Am 5' ends and determined the
238 GFP signal by microscopy and flow cytometry (Figure 7A and S8). Although both
239 mRNAs are transfected with similar efficiencies, m6Am-EGFP transfected cells showed
240 diminished GFP signal (Figures 7A-D and S8), suggesting that m6Am-containing
241 transcripts are translated less efficiently that the unmethylated counterparts *in vivo*. To
242 further validate the effect of m6Am on translation and to investigate whether this effect
243 is independent of the mRNA sequence, we performed *in vitro* translation assays using
244 varying amounts of firefly luciferase mRNAs with cap adjacent Am or m6Am
245 modifications, followed by luminometric quantification. Similar to our *in vivo* reporter
246 assays, m6Am suppressed translation of luciferase mRNA *in vitro* (Figure 7E). Next, we
247 investigated whether m6Am-mediated suppression is specific to cap-dependent
248 translation by employing Am or m6Am methylated bi-cistronic mRNA transcripts in *in*
249 *vitro* translation assays. m6Am suppressed the translation of cap-dependent firefly
250 luciferase whereas IRES mediated translation of renilla luciferase was unaffected,
251 indicating that m6Am specifically suppresses cap-dependent translation (Figure 7F).

252

253 Given that m6Am is a cap proximal RNA modification that suppresses cap-dependent
254 translation we next determined whether m6Am affects the interaction between mRNA
255 and cap binding protein eIF4E. Specifically, we analyzed binding dynamics between
256 recombinant human eIF4E protein and capped Am and m6Am RNA oligos, as well as
257 de-capped RNA oligos, by microscale thermophoresis (MST). As expected, the affinity
258 of eIF4E to the RNA decreased significantly when the mRNA cap was removed.
259 Importantly, we found that m6Am also decreased the affinity of eIF4E to the capped
260 RNA oligo, in comparison to capped Am RNA (Figure S9). Taken together, these data
261 suggest that m6Am modification suppresses cap-dependent mRNA translation, possibly
262 by decreasing eIF4E binding.

263

264 **Discussion**

265 In this study, we uncovered a new regulatory mechanism mediated by PCIF1 m6Am
266 deposition on mRNAs. Our *in vivo* and *in vitro* data demonstrate that PCIF1 is the only
267 methyltransferase necessary and sufficient for the conversion of cap-Am mRNAs to
268 cap-m6Am mRNAs in human cells. Moreover, we provide evidence that m6Am
269 negatively regulates cap dependent translation by decreasing the binding of eIF4E to
270 m6Am-containing transcripts. Our findings highlight a previously unknown translational
271 regulatory pathway that begins with a modification in the nucleus, opening new avenues
272 of investigation in the epitranscriptome and translation fields.

273

274 Given that m6Am marks diverse transcripts including noncoding snRNAs and histone
275 mRNAs that are translated independently of eIF4E, we predict that this modification will
276 play diverse functions, which include but are not limited to protein translation. m6Am
277 has been suggested to play a role in regulating the stability of modified mRNAs in
278 HEK293T cells (Mauer et al., 2017) . However, our analyses show that neither
279 transcription nor abundance of m6Am-enriched transcripts are affected in PCIF1 KO
280 MEL624 cells (Figure 6). However, we cannot rule out a potential role of m6Am in
281 regulating mRNA stability under conditions that were not tested in this study.

282

283 Rather than altering mRNA stability, we found that m6Am suppresses cap dependent
284 translation, possibly by reducing binding of eIF4E to the capped mRNAs. Our findings
285 strongly suggest a role for PCIF1 in protein translation control, which will be validated by

286 investigation of translation of endogenous mRNAs by PCIF1. Collectively, the
287 identification of PCIF1 as the sole, evolutionarily conserved, mRNA m6Am
288 methyltransferase paves the way for investigating the impact of PCIF1 on gene
289 expression of m6Am-marked transcripts in diverse biological contexts.
290

Acknowledgments

We thank members of the Shi lab for helpful discussions. We are especially indebted to the Tufts Genomic Core and Karla F Meza-Sosa for helpful advice and reagents. We thank Synaptic Systems for kindly providing m6A antibodies. This work was supported by a grant from the NIH to Y.S. (R01 GM117264), funds from Boston Children's Hospital to Y.S. and Startup Funds provided by Harvard Medical School to K.A. Y.S. is an American Cancer Society Research Professor. This work used the Extreme Science and Engineering Discovery Environment (XSEDE), which is supported by NSF grant number ACI-1548562. Specifically, it used the Bridges system, which is supported by NSF award number ACI-1445606, at the Pittsburgh Supercomputing Center (PSC). D.V-G. is supported by a postdoctoral fellowship from the Mexican Council of Science and Technology (CONACYT, CVU: 257385) and is a member of the Mexican National System of Researchers (SNI I).

Author contributions:

E.S., D.V-G. and Y.S. conceived and designed the study. E.S., D.V-G., A.D., H.C., T.H. and W.S. performed the research. T.H. and K.A. performed and analyzed PRO-Seq. E.S., D.V-G. and Y.S. wrote the manuscript and all authors contributed to the final version of the manuscript.

313 **Declaration of interests**

314 Y.S. is a cofounder of Constellation Pharmaceuticals and Athelas Therapeutics, and a
315 consultant for Active Motif, Inc.

316

317 **Data availability**

318 Once the paper is published, all the genome-wide data will be accessible through GEO
319 with accession number GSE122803.

320

321 **References**

322 Dominissini, D., Moshitch-Moshkovitz, S., Schwartz, S., Salmon-Divon, M., Ungar, L.,
323 Osenberg, S., Cesarkas, K., Jacob-Hirsch, J., Amariglio, N., Kupiec, M., et al. (2012).
324 Topology of the human and mouse m6A RNA methylomes revealed by m6A-seq.
325 Nature *485*, 201–206.

326 Ebmeier, C.C., Erickson, B., Allen, B.L., Allen, M.A., Kim, H., Fong, N., Jacobsen, J.R.,
327 Liang, K., Shilatifard, A., Dowell, R.D., et al. (2017). Human TFIIH Kinase CDK7
328 Regulates Transcription-Associated Chromatin Modifications. Cell Rep. *20*, 1173–1186.

329 Fan, H., Sakuraba, K., Komuro, A., Kato, S., Harada, F., and Hirose, Y. (2003). PCIF1,
330 a novel human WW domain-containing protein, interacts with the phosphorylated RNA
331 polymerase II. Biochem. Biophys. Res. Commun. *301*, 378–385.

332 Hirose, Y., Iwamoto, Y., Sakuraba, K., Yunokuchi, I., Harada, F., and Ohkuma, Y.
333 (2008). Human phosphorylated CTD-interacting protein, PCIF1, negatively modulates
334 gene expression by RNA polymerase II. Biochem. Biophys. Res. Commun. *369*, 449–
335 455.

336 Iyer, L.M., Zhang, D., and Aravind, L. (2016). Adenine methylation in eukaryotes:
337 Apprehending the complex evolutionary history and functional potential of an epigenetic
338 modification. Bioessays *38*, 27–40.

339 Keith, J.M., Ensinger, M.J., and Moss, B. (1978). HeLa Cell RNA(2'-0-methyladenosine-
340 W-)-methyltransferase Specific for the Capped &End of Messenger RNA*.

341 Kruse, S., Zhong, S., Bodi, Z., Button, J., Alcocer, M.J.C., Hayes, C.J., and Fray, R.
342 (2011). A novel synthesis and detection method for cap-associated adenosine

343 modifications in mouse mRNA. Sci. Rep. *1*, 126.

344 Kwak, H., Fuda, N.J., Core, L.J., and Lis, J.T. (2013). Precise maps of RNA polymerase

345 reveal how promoters direct initiation and pausing. Science *339*, 950–953.

346 Linder, B., Grozhik, A. V, Olarerin-George, A.O., Meydan, C., Mason, C.E., and Jaffrey,

347 S.R. (2015). Single-nucleotide-resolution mapping of m6A and m6Am throughout the

348 transcriptome. Nat. Methods *12*, 767–772.

349 Mauer, J., Luo, X., Blanjoie, A., Jiao, X., Grozhik, A. V., Patil, D.P., Linder, B., Pickering,

350 B.F., Vasseur, J.-J., Chen, Q., et al. (2017). Reversible methylation of m6Am in the 5′

351 cap controls mRNA stability. Nature *541*, 371–375.

352 Mauer, J., Sindelar, M., Guez, T., Vasseur, J.-J., Rentmeister, A., Gross, S., Pellizzoni,

353 L., Debart, F., Goodarzi, H., and Jaffrey, S.R. (2018). The RNA demethylase FTO

354 targets m 6 Am in snRNA to establish distinct methyl isoforms that influence splicing.

355 Meyer, K.D., Saletore, Y., Zumbo, P., Elemento, O., Mason, C.E., and Jaffrey, S.R.

356 (2012). Comprehensive analysis of mRNA methylation reveals enrichment in 3' UTRs

357 and near stop codons. Cell *149*, 1635–1646.

358 Sonenberg, N., and Gingras, A.C. (1998). The mRNA 5' cap-binding protein eIF4E and

359 control of cell growth. Curr. Opin. Cell Biol. *10*, 268–275.

360 Tomoo, K., Shen, X., Okabe, K., Nozoe, Y., Fukuhara, S., Morino, S., Ishida, T.,

361 Taniguchi, T., Hasegawa, H., Terashima, A., et al. (2002). Crystal structures of 7-

362 methylguanosine 5'-triphosphate (m(7)GTP)- and P(1)-7-methylguanosine-P(3)-

363 adenosine-5',5'-triphosphate (m(7)GpppA)-bound human full-length eukaryotic initiation

364 factor 4E: biological importance of the C-terminal flexible region. Biochem. J. *362*, 539–

365 544.

366 Tomoo, K., Matsushita, Y., Fujisaki, H., Abiko, F., Shen, X., Taniguchi, T., Miyagawa,
367 H., Kitamura, K., Miura, K.-I., and Ishida, T. (2005). Structural basis for mRNA Cap-
368 Binding regulation of eukaryotic initiation factor 4E by 4E-binding protein, studied by
369 spectroscopic, X-ray crystal structural, and molecular dynamics simulation methods.
370 Biochim. Biophys. Acta *1753*, 191–208.

371 Wei, C.M., Gershowitz, A., and Moss, B. (1975). N6, O2'-dimethyladenosine a novel
372 methylated ribonucleoside next to the 5' terminal of animal cell and virus mRNAs.
373 Nature *257*, 251–253.

374 Wei, J., Liu, F., Lu, Z., Fei, Q., Ai, Y., He, P.C., Shi, H., Cui, X., Su, R., Klungland, A., et
375 al. (2018). Differential m6A, m6Am, and m1A Demethylation Mediated by FTO in the
376 Cell Nucleus and Cytoplasm. Mol. Cell *71*, 973–985.e5.

377 Yang, Y., Hsu, P.J., Chen, Y.-S., and Yang, Y.-G. (2018). Dynamic transcriptomic m6A
378 decoration: writers, erasers, readers and functions in RNA metabolism. Cell Res. *28*,
379 616–624.

380

381 **Figures**

382

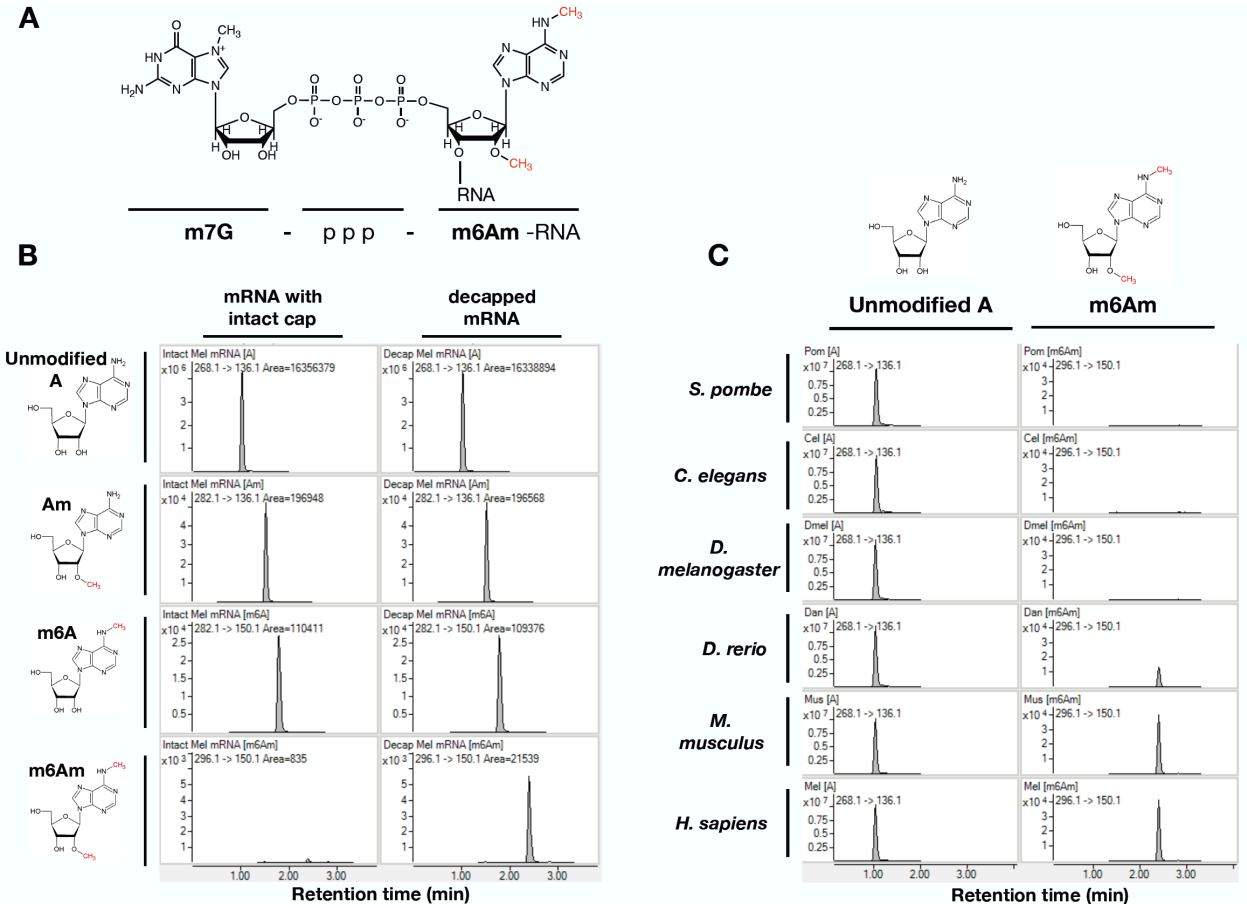

383
384

385 **Figure 1. m6Am is an evolutionarily conserved RNA modification that is restricted to 5'**
386 **end of mRNAs**

387

388 1A. Chemical structure of 5' end of eukaryotic mRNA with m6Am methylation.
389 1B. MS spectra of mRNA from MEL624 human melanoma cell line with or without treatment by
390 de-capping enzyme to remove m7G cap prior to digestion for MS analysis. m6Am is detectable
391 only when mRNA is de-capped.
392 1C. MS spectra of de-capped mRNAs isolated from indicated organisms.

393

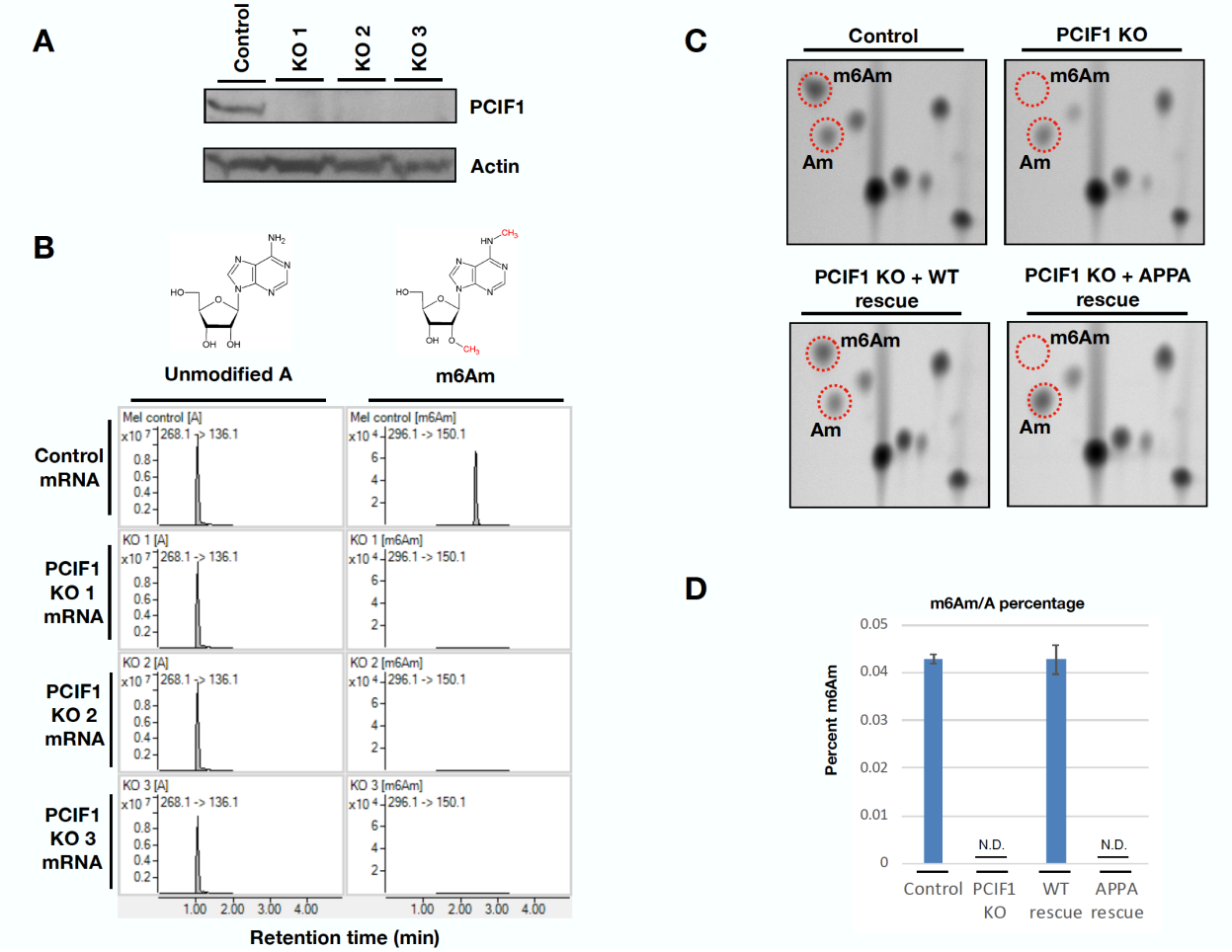

Figure 2. PCIF1 is required for mRNA m6Am methylation *in vivo*

2A. Western blot analysis of control and three independent PCIF1 KO MEL624 cell lines with antibodies against endogenous PCIF1. Beta-actin is shown as a loading control.
2B. MS spectra of de-capped mRNA from control and three independent PCIF1 KO MEL624 cell lines.
2C. Thin-layer chromatography analysis of cap-adjacent nucleotides from mRNA isolated from control, PCIF1 KO and KO cells rescued with wild type or catalytic mutant PCIF1 (APPA).
2D. HPLC-MS/MS m6Am/A percentages of mRNAs from control, PCIF1 KO and KO cells rescued with wild type or catalytic mutant PCIF1 (APPA). (N.D., Not Detected). (n=3). Error bars depict standard error.

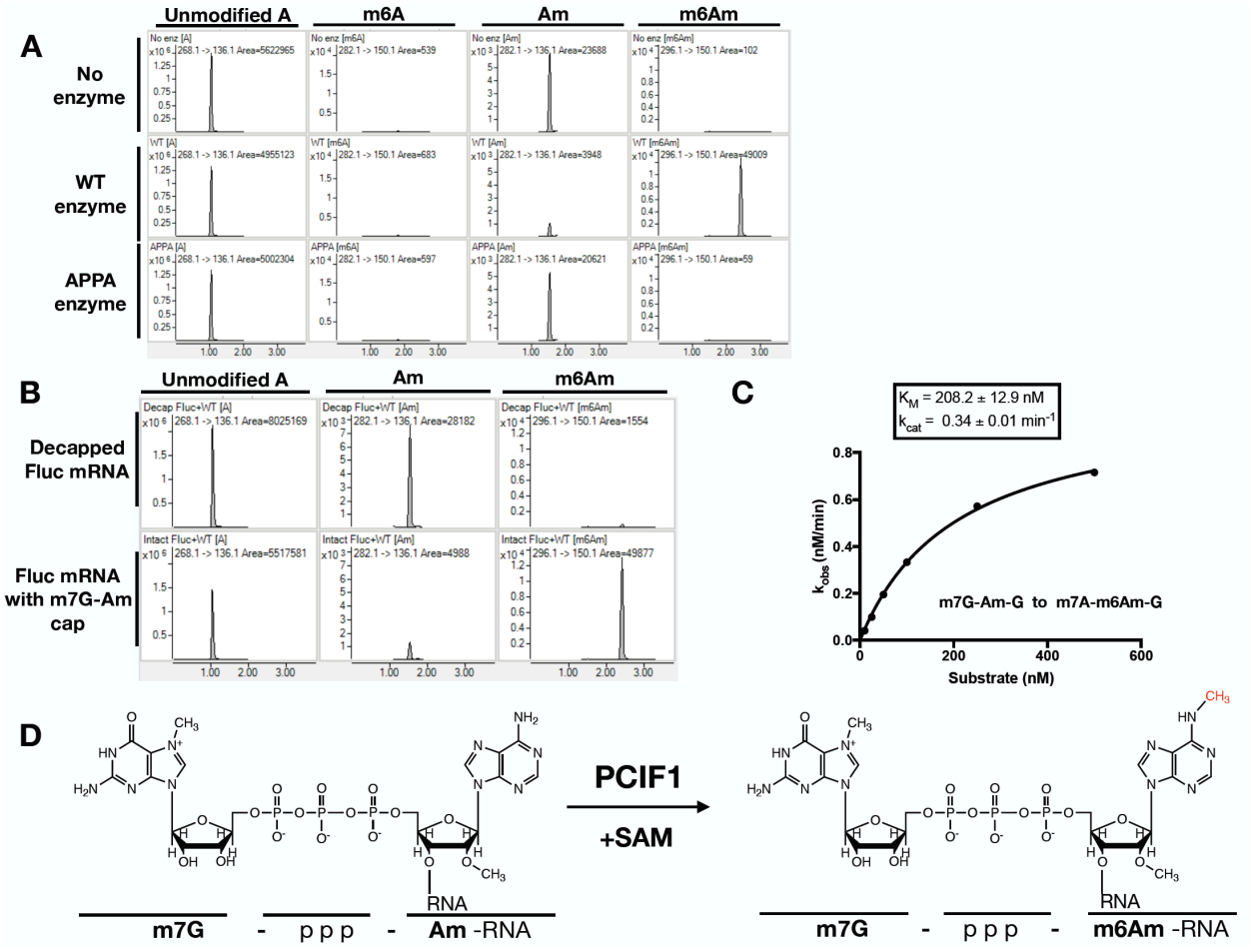

Figure 3. Recombinant PCIF1 methylates capped mRNA *in vitro*.

3A. Firefly luciferase mRNA with m7G-Am cap structure is methylated with wild-type or catalytic mutant recombinant PCIF1 *in vitro*. The methylation pattern of mRNA was analyzed by LC-MS/MS.

3B. In vitro methylation assays were performed with recombinant PCIF1 enzyme using de-capped firefly luciferase mRNA or mRNA with intact m7G-Am cap.

3C. Michaelis–Menten kinetics of recombinant PCIF1 was determined using m7G-Am capped dinucleotide RNA oligo by LC-MS/MS analysis.

3D. Chemical structures of PCIF1 substrate and product.

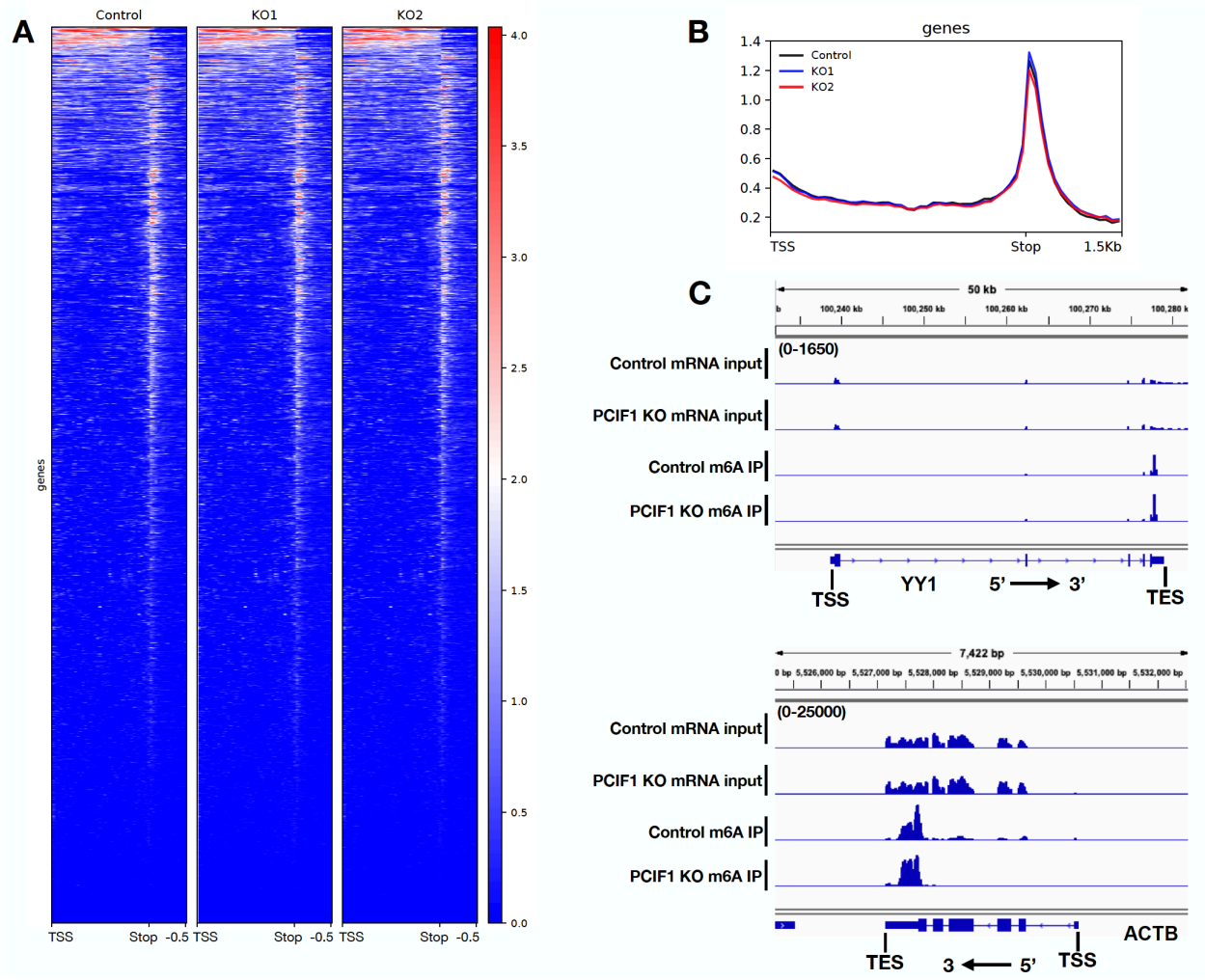

Figure 4. Loss of PCIF1 does not affect global mRNA m6A distribution *in vivo*.

4A. Heat map of m6A enrichment over Input of genes overlapping with m6A peaks (n=4,460) in MEL624 cell line determined by m6A MeRIP-Seq in control and two independent PCIF1 KO cell lines.

4B. Metagene plots of m6A enrichment over Input of genes overlapping with m6A peaks (n=4,460) in MEL624 cell line determined by m6A MeRIP-Seq in control and two independent PCIF1 KO cell lines.

4C. Genome browser views of two examples genes with m6A enrichment near stop codon.

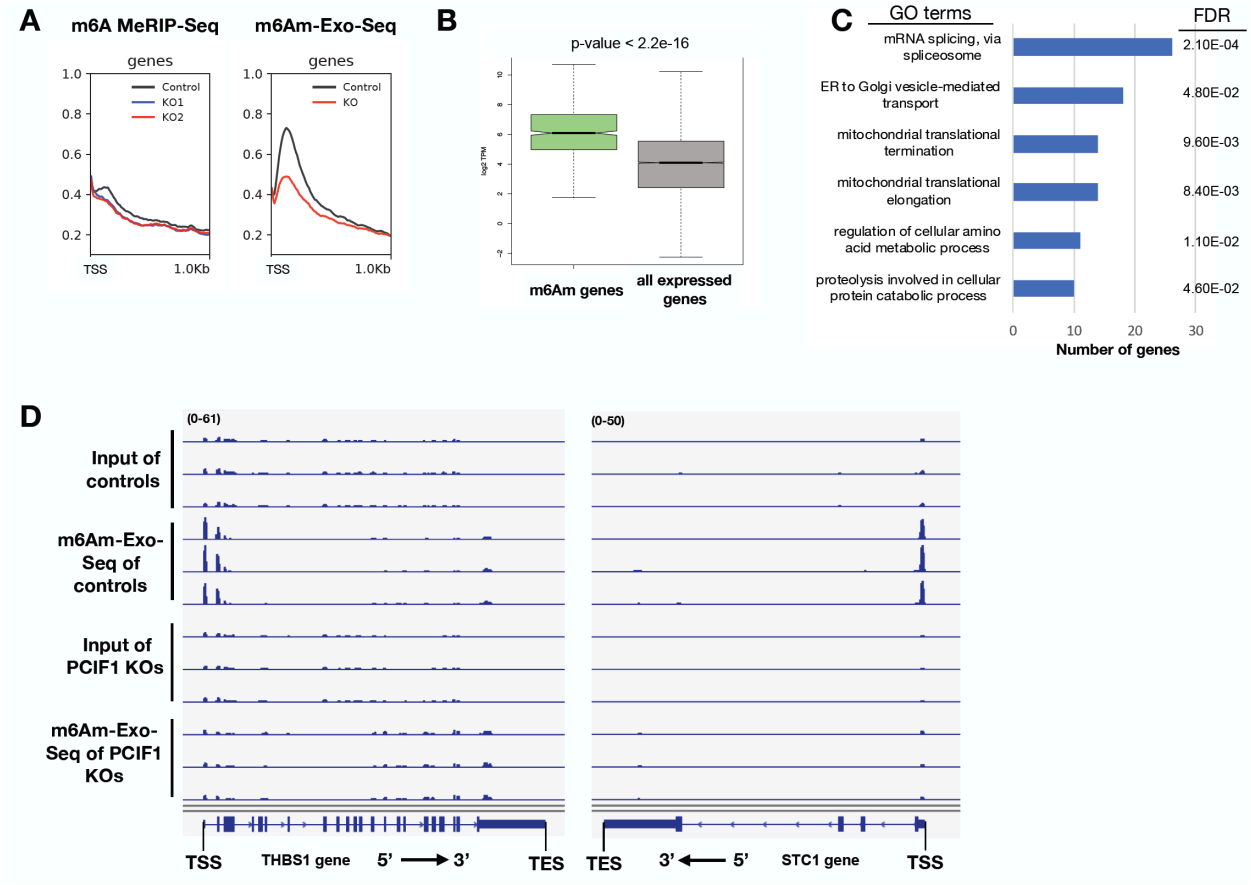

Figure 5. m6Am-Exo-Seq as a robust methodology that enables global m6Am mapping.

5A. Metagene plots of m6A(m) enrichment over Input near TSS of all expressed genes (n=15,258) in MEL624 cells employing either m6A MeRIP-Seq or m6Am-Exo-Seq methodology in control and PCIF1 KO cells.
5B. Boxplots of expression level (log2 TPM) of m6Am mRNAs (n=640) vs. all mRNAs expressed in MEL624 cell line (n=15,258). The observed difference is significant (p-value < 2.2e-16) using a Mann-Whitney test. Box plots show the 25th–75th percentiles and error bars depict the 10th–90th percentiles.
5C. Biological process Gene Ontology (GO) terms that have FDR<0.05 identified by DAVID 6.8
5D. Genome browser views of 2 example genes with m6Am enrichment using m6Am-Exo-Seq

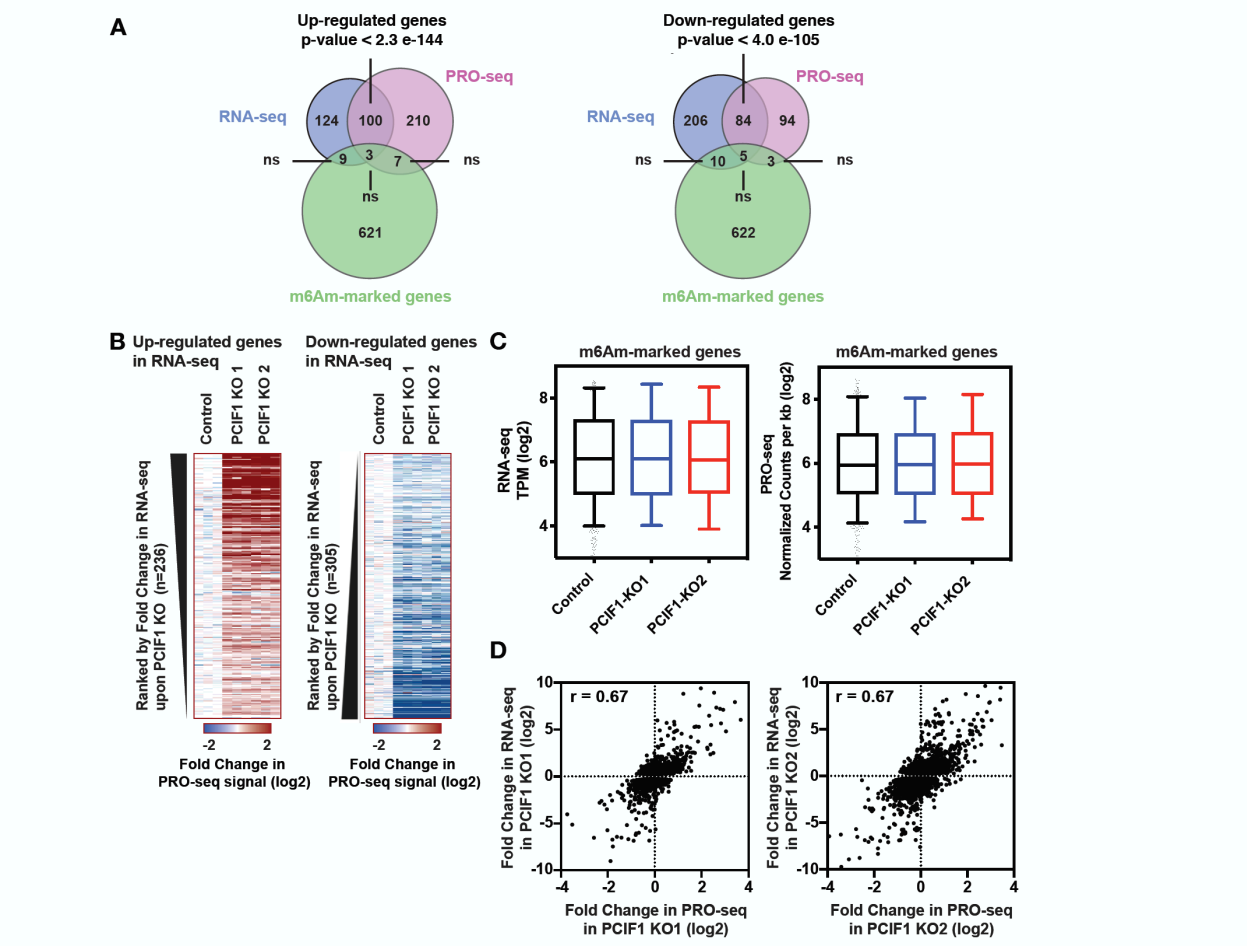

Figure 6. PCIF1-mediated deposition of m6Am does not alter transcription or stability of target genes.

6A. Venn diagrams displaying overlap between m6Am-enriched genes in MEL624 cells and genes identified as significantly upregulated (left) or downregulated (right) in both PCIF1 KO MEL624 cell lines, by RNA-Seq and PRO-Seq. P-values are calculated with a hypergeometric test.

6B. Heatmaps of PRO-Seq signal at genes found to be up- or down-regulated using RNA-Seq in PCIF1 KO cells. Shown are the fold changes in PRO-Seq signal across the bodies of genes up-regulated in RNA-Seq (left) or down-regulated in RNA-Seq (right). Genes are ranked from most upregulated to least (at left) and least down-regulated to most (at right), demonstrating that PRO-Seq signal scales with results from RNA-seq.

6C. RNA-Seq signal (left) and normalized PRO-Seq signal (right) within 640 m6Am-enriched genes in Control MELF624 cells, as compared to PCIF1 KO cells. Box plots show the 25th–75th percentiles and error bars depict the 10th–90th percentiles. Differences are not significant ($P > 0.01$). P-values were calculated using the Mann-Whitney test.

6D. Scatter plots displaying the correlation of RNA-Seq vs PRO-Seq KO/control fold change signal. Only genes that have a fold change > 1.2 according to RNA-Seq in KO1 or KO2 were plotted. The total number of genes used in KO1 plot is 5,774 and KO2 is 5,580. Both KOs have the same Pearson correlation value of 0.67.

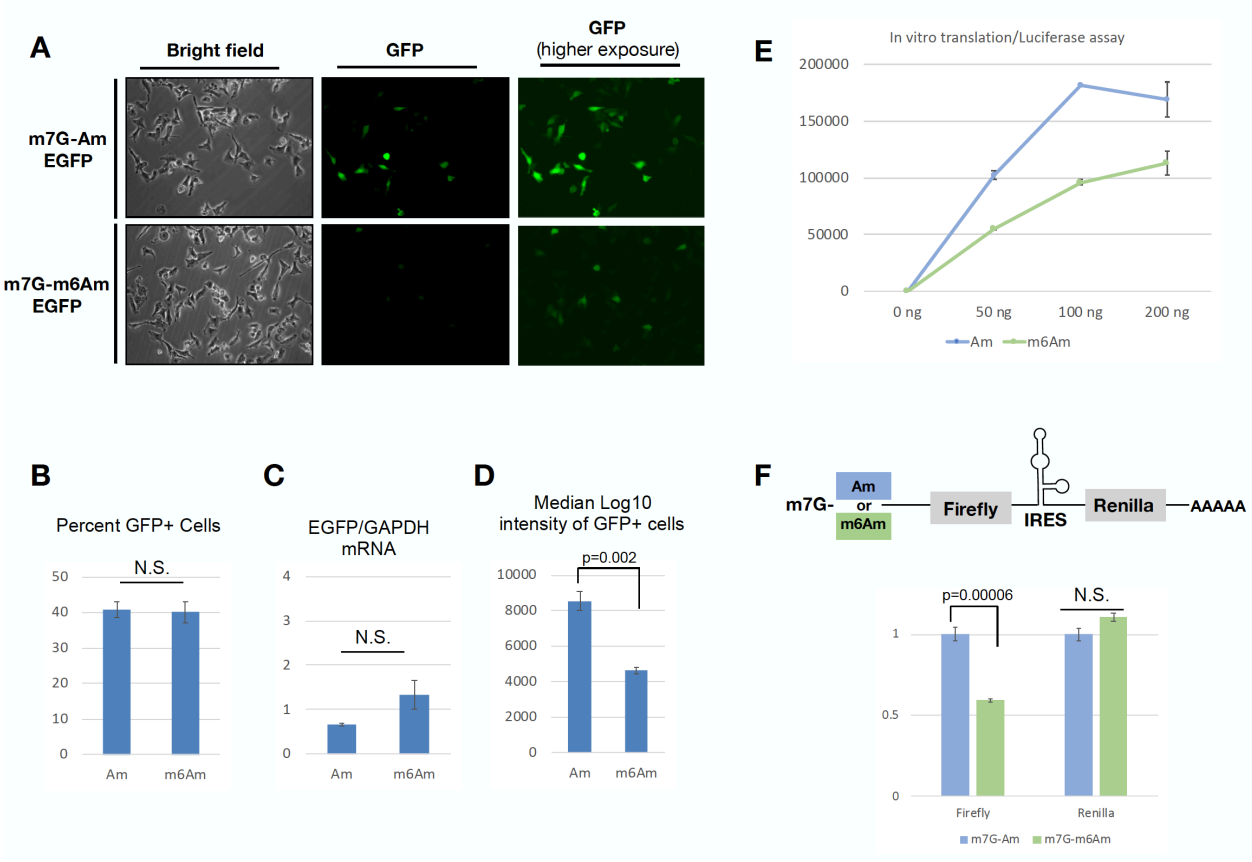

Figure 7. m6Am suppresses cap-dependent translation.

7A. EGFP mRNA that starts with either m7G-Am or m7G-m6Am was transfected into PCIF1 KO MEL624 cells. GFP signal was determined by fluorescence microscopy 24 hours post-transfection.
7B. The percentage of GFP positive cells from the experiment in 7A determined by flow cytometry (n=3 replicates).
7C. EGFP mRNA level from the cells in experiment 7A as determined by RT-qPCR. (n=3 replicates).
7D. Median fluorescence intensity of the cells from the experiment in 7A determined by flow cytometry. P-values in 7B-D are calculated using unpaired t-tests. (n=3 replicates).
7E. *In vitro* translation assays were carried out with indicated amounts of luciferase mRNA starting with m7G-Am or m7G-m6Am using rabbit reticulocyte system. Resulting luciferase signal was quantified on a plate reader. (n=4 replicates)
7F. In vitro translation assays were carried out with bicistronic construct that starts with m7G-Am or m7G-m6Am using rabbit reticulocyte system. Resulting firefly and renilla luciferase signals were quantified on a plate reader. (n=4 replicates). The p-values were calculated with an unpaired t-test. All error bars in this figure depict standard error.

491 **Methods**

492

493 **Cell culture**

494 MEL624 (RRID: CVCL_8054) and HEK293T (RRID:CVCL_0063) cells are grown in
495 DMEM (Gibco) supplemented with 10% FBS and 1x pen/strep solution (Gibco) at 37ºC
496 in a CO_2 incubator. Cells are split once they reach ~90% confluence with a 1:8 ratio.
497 Cells are routinely checked for mycoplasma infection.

498

499 **mRNA purification**

500 Total RNA is isolated from MEL624 cells with TRIzol reagent following manufacturer's
501 instructions. 200 μg of total RNA are subjected to two rounds of Poly(A) mRNA
502 purification using the magnetic mRNA isolation kit from (NEB). 100 μL of oligo d(T)
503 magnetic beads are used per purification. mRNA is eluted in a final volume of 50 μL, in
504 elution buffer.

505

506 **Processing of RNA Samples for Mass Spectrometry**

507 250 or 500 ng of mRNA is de-capped with a decapping enzyme in 20 μL reaction
508 volume for an hour at 37ºC. Then the RNA is digested with 0.5U of nuclease P1 (Sigma)
509 in P1 buffer in 50 uL reaction at 37^{oo}C for 2 hours. To dephosphorylate the single
510 nucleotides, 1U of rSAP (NEB) is added to a final reaction volume of 100 μL with
511 CutSmart buffer (NEB) and incubated for an hour at 37^{oo}C. The 100 μL samples are
512 filtered with Millex-GV 0.22u filters.

513 **HPLC-MS/MS Analysis**

514 10 uL from each sample is injected into Agilent 6470 Triple Quad LC/MS instrument.
515 The samples are run in mobile phase buffer A (water with 0.1% Formic Acid) and 2 to
516 20% gradient of buffer B (Methanol with 0.1% Formic Acid). MRM transitions are
517 measured for adenosine (268.1 to 136.1, retention time 1.03 min), guanosine (284.1 to
518 152.1, retention time 1.15 min), 2'-O-methyladenosine (Am) (282.1 to 136.1, retention
519 time 1.52 min), N6-methyladenosine (m6A) (282.1 to 150.1, retention time 1.79 min),
520 N6,2-O-dimethyladenosine (m6Am) (296.1 to 150.1, retention time 2.40 min). The
521 concentrations of each compound in the samples are calculated using calibration curves
522 constructed with standard compounds of adenosine (Abcam), N6-methyladenosine
523 (Abcam), N6,2'-O-dimethyladenosine (Toronto Research Chemicals). For LC/MS-MS
524 data collection and analysis, Agilent Mass Hunter LC/MS Data Acquisition Version
525 B.08.00 and Quantitative Analysis Version B.07.01 softwares are used.

526

527 **mRNA purification from different species**

528 Total RNA was extracted with TRIzol from the following sources:
529 Human: MEL624 melanoma cell line (RRID: CVCL_8054)
530 Mouse: C2C12 mice myoblast cell line (ATCC Cat# CRL-1772, RRID:CVCL_0188)
531 Zebrafish: WT adult whole fish (ZFIN Cat# ZDB-GENO-990623-3, RRID:ZFIN_ZDB-
532 GENO-990623-3)
533 Worm: Adult N2 (WT) *C. elegans* (WB Cat# N2, RRID:WB-STRAIN:N2)
534 Fly: KC drosophila cell line (RRID:CVCL_Z833)

535 Yeast: *S. pombe*, ED666 h+ ade6-M210 ura4-D18 leu1-32 from Bioneer Inc.

536 mRNA was extracted from 50-100 μg of total RNA as described above.

537

538 **Generation of PCIF1 KO cell lines**

539 Two complementary strategies are followed to generate clonal PCIF1 MEL624 cell lines.

540 3 sgRNAs were cloned into the lentiCRISPR V2 vector (RRID:Addgene_52961):

541 PCIF1 sgRNA-1: TAGCGGTAAAGGAGCCACTG

542 PCIF1 sgRNA-2: CGGTTGAAAGACTCCCGTGG

543 PCIF1 sgRNA-3: ATTCACCAACCAGTCCCTGT

544 Additionally, a random non-targeting sgRNA was cloned into lentiCRISPR V2 as a

545 control:

546 Random sgRNA-1: ATCGTTTCCGCTTAACGGCG

547 For the first strategy, 1 μg of lentiCRISPR V2 plus 0.5 μg of psPAX2

548 (RRID:Addgene_12260) and 0.2 μg of pMD2.G (RRID:Addgene_12259) packaging

549 plasmids were mixed with 3 μg of polyethylenimine (PEI) in 100 ul of OptiMEM (Gibco)

550 and added into 6-well plates of 30% confluent HEK293T cells (RRID:CVCL_0063). 4

551 hours post-transfection, the transfection media was replaced with 1.5 mL of regular

552 media (DMEM, 10% FBS, 1X pen/strep). 48 hours post-transfection the media

553 containing viral particles was passed through a 0.45 um filter and the viral particles from

554 the 3 PCIF1 sgRNAs were combined. 200 μL of the pooled viral particles were used to

555 infect a 6-well plate of ~30% confluent MEL624. At the same time, another 6-well plate

556 was infected with 200 μl from the non-targeting sgRNA. Under these conditions we

557 reached an infection rate of ~50%. 12 hours post-infection, cells were washed with PBS
558 and media with 1 μg/mL of puromicyn was added to select infected cells. 48 hours post-
559 selection, cells were grown with regular media for additional 48 hours and single-cell
560 sorted in a 96-well plate in a FACS Aria cell sorter. Individual clones were validated as
561 true KOs by western blot with a PCIF1 specific antibody (Bethyl A304-711A). This
562 strategy generated PCIF1 KO1 and PCIF1 KO2 cell lines, as well as the control cell line
563 from the non-targeting sgRNA clones.
564
565 In the second strategy, and to avoid integration of cas9 into the genome, 2 μg of
566 lentiCRISPRv2 from the PCIF1 sgRNA-2 were transfected into a ~30% confluent 6-well
567 plate of MEL624 cells using 4 μl of lipofectamine 2000 according to manufacturer's
568 instructions. 24 hours post-transfection, cells were selected with 1 μg/mL of puromycin
569 for 48 hours and growth for additional 48 hours without selection. Cells were single-cell
570 sorted and evaluated as described above. This strategy generated the PCIF1 KO used
571 for the rescues and m6Am mapping experiments.
572
573 **PCIF1 KO cell line rescue**
574 WT and catalytic-deficient versions of PCIF1 coding sequence were cloned into the
575 PHAGE-puro lentiviral plasmid with a C-terminal HA-FLAG tag. Lentiviruses were
576 prepared as described above. 500 μL of lentiviral particles were used to infect ~30%
577 confluent MEL624 KO cells. 12 hours post-infection, viruses were washed out with PBS
578 and cells were selected with media containing 1 μg/mL of puromycin for 48 hours. After

579 selection, rescue cell lines were continuously growth in media containing 0.5 μg/mL of
580 puromycin to avoid the silencing of PCIF1 transgene.
581
582 **PCIF1 immunofluorescence**
583 PCIF1 KO and rescue cell lines were seeded in a 96-well plate to a ~70% confluence.
584 Cells are fixed for 10 mins in 3.7% formaldehyde in PBS at room temperature. Cells are
585 washed twice with PBS and permeabilized for 10 mins with 0.1% saponin in PBS. Cells
586 are blocked at room temperature for 1 hour with IF blocking buffer (10% BSA, 0.3%
587 triton in PBS) and then are incubated overnight at 4ºC with a monoclonal anti-FLAG
588 antibody (Sigma-Aldrich Cat #F1804, RRID:AB_262044) diluted 1:500 in IF buffer (10%
589 FBS, 1% BSA, 0.3% triton in PBS). Primary antibody is washed three times with 0.05%
590 PBS-Tween. Cells are incubated with Alexa 488 goat anti-Mouse (Thermo Fisher
591 Scientific Cat #A-11029, RRID:AB_2534088) 1:1000 in IF buffer for 1 h at room
592 temperature in the dark. DAPI is added to a final concentration of 0.2 μg/mL and
593 incubated for additional 10 mins. Cells are washed three times with 0.05% PBS-Tween,
594 once with PBS and then imaged in a Nikon Eclipse Ti fluorescent microscope. Pictures
595 of representative fields are taken with a S Plan Fluor 20X/0.45 objective with the NIS
596 Elements v4.20 software (DAPI channel exposure: 500 msec. GFP channel exposure:
597 600 msec.).
598
599
600

601 **Thin Layer Chromatography**

602 1 μg of mRNA is cleaned, labeled and digested as previously described (Kruse et al.,
603 2011; Mauer et al., 2017). 10% of the starting material is loaded into a TLC cellulose
604 glass plate and first and second dimensions are run for 14 and 19 hours, respectively.
605 Plates are exposed to a phosphor imager screen for 24 hours and read in a Typhoon
606 scanner. Pictures are analyzed and quantified using Fiji v2.0.0 (RRID:SCR_002285).

607

608 **Recombinant Protein Purification**

609 Full-length human PCIF1 gene is cloned into pGEX-4T1 vector. It is expressed
610 overnight in 500 mL Rosetta bacteria (Novagen) culture induced with 0.1 mM IPTG at
611 18°C. The cells are lysed in 15 mL cold lysis buffer (50 mM Tris pH 7.4, 150 mM NaCl,
612 0.05% NP-40, 1mM PMSF) with 0.25 mg/mL chicken lysozyme on ice for 30 min. The
613 cell lysate is sonicated on ice and cleared with centrifugation for 20 min at 10000 rpm at
614 4°C. The GST tagged recombinant protein is bound to Glutathione Sepharose 4B beads
615 (GE Healthcare) at 4°C with rotation for 3 hours. The beads are washed with lysis buffer
616 containing 500 mM NaCl. The untagged recombinant protein is eluted off the beads with
617 overnight rotation at room temperature with 5U of thrombin in thrombin cleavage buffer
618 (50 mM Tris pH 8.0, 150 mM NaCl, 5mM $CaCl_2$). The protein preparation is
619 supplemented with 10% glycerol and stored at -80°C.

620

621 Full-length human EIF4E gene with N terminal 6xHis tag is cloned into pGEX-4T1
622 vector. The same purification protocol for recombinant PCIF1 is followed with the

623 following exceptions. The initial lysis buffer is supplemented with 10U RNaseA/T1 mix.
624 The cleared lysate is first bound to Ni-NTA beads at 4°C for 3 hours to purify using the
625 6xHis tag, washed in lysis buffer with 750 mM NaCl and eluted in His elution buffer (50
626 mM Tris pH 7.4, 150 mM NaCl, 150 mM imidazole). The eluted protein is bound to
627 Glutathione Sepharose 4B beads (GE Healthcare) at 4°C with rotation for 1 hour and
628 eluted off the beads with overnight rotation at room temperature with 5U of thrombin in
629 thrombin cleavage buffer (50 mM Tris pH 8.0, 150 mM NaCl, 5mM $CaCl_2$). The protein
630 preparation is supplemented with 10% glycerol and stored at -80°C.
631

632 **Enzyme Kinetics**

633 The enzymatic parameters for m7G-Am methylation were determined by incubating full-
634 length untagged recombinant PCIF1 enzyme (3 nM) with increasing concentrations of
635 RNA dinucleotide (10 – 500 nM) at 37 C in 50 mM Tris-HCl (pH 7.5 @ 25 °C), 5 mM β-
636 ME, 10 mM EDTA and 80 µM S-adenosylmethionine (SAM) buffer. Aliquots were
637 withdrawn at t = 0, 2, 5, 10, 30 and 60 min and boiled for 3 min to stop all enzymatic
638 activity. The aliquots were further processed as described in Processing of RNA
639 samples for mass spectrometry methods section. The levels of the final product (m7G-
640 m6AmG) formed at each time point was determined using mass spectrometry by
641 monitoring the amount of m6Am in each aliquot. The observed rate of product formation
642 (kobs) was determined by plotting the concentration of m6Am against time for each
643 concentration of the substrate (10, 25, 50, 100, 250, 500 nM). The kobs vs substrate
644 concentration curve was fit to the Michaelis-Menten equation using the Graphpad Prism

645 software to obtain the final enzymatic parameters. The same protocol was followed for
646 kinetics using EGFP mRNA with indicated concentrations.
647
648 ***In vivo* translation assays**
649 200 ng of either Am-, or m6Am-EGPF mRNA are transfected into a 6-well plate with
650 MEL624 at ~30% confluence. Transfection is done with 1 μl of lipofectamin 2000
651 according to manufacturer's instructions. Untransfected wells are used as negative
652 controls. 24 h post-transfections, cells are imaged in a Nikon Eclipse Ti fluorescent
653 microscope and pictures of representative fields are taken with a S Plan Fluor 20X/0.45
654 objective with the NIS Elements v4.20 software (GFP channel low exposure: 500 msec.
655 GFP channel high exposure: 3 sec. bright field exposure: 20-40 msec.). At the same
656 time, a second set of transfected wells is trypsinized, washed once with PBS and
657 resuspended in 500 μl of PBS for flow cytometry. Cells are analyzed in a FACS Canto II
658 and percentages of GFP positive cells as well as GFP intensity values are calculated
659 with FloJo 8.7. Finally, a third set of transfected wells is lysed with 200 μL of TRIzol and
660 total RNA is purified following manufacturer's instructions. Quantitative PCR is
661 performed with primers specific for GFP and GAPDH as internal control in order to
662 determine the level of mRNA that was transfected into the cells.
663
664 ***In vitro* Translation**
665 In vitro translation reactions are carried out using Retic Lysate IVT kit (Invitrogen
666 Ambion) in 25 μL or 10 μL reactions with varying indicated mRNA concentrations (50,

667 100 or 200 ng). The translation is carried out at 30°C for 1 hour. For the firefly luciferase
668 mRNA translation reactions, luciferase reagent supplied by Firefly Luc One-Step Glow
669 Assay Kit (Pierce Thermo Fisher Scientific) is used. For the in vitro transcribed
670 bicistronic firefly-IRES-renilla luciferase mRNA translation reactions, luciferase reagents
671 supplied by Dual-Luciferase Reporter Assay System (Promega) are used and
672 luminescence is measured on a plate reader.
673
674 **m6A MeRIP-Seq**
675 m6A MeRIP experiments were performed following the recommendations from the
676 EpiMark N6-Methyladenosine Enrichment Kit (NEB #E1610). Briefly: 10 μg of mRNA
677 were incubated at 98ºC for 3 min in fragmenting buffer (10 mM Tris pH 7.4, 10 mM
678 $ZnCl_2$) to generate fragments of ~100-150 bp. Fragmented RNA is incubated with
679 protein G magnetic beads conjugated to 1 μL (250 μg) of anti-m6A rabbit monoclonal
680 antibody from the EpiMark kit for 1 h at 4ºC. Beads were washed twice with 200 μL of
681 reaction buffer, twice with 200 μL of low salt buffer and twice with 200 μL of high salt
682 buffer. Immunoprecipitated RNA was eluted with TRIzol and purified. Illumina
683 sequencing libraries are prepared with the NEBNext Ultra II Directional Library Prep Kit
684 for Illumina from NEB (#E7760), following manufacture's instructions. RNA-Seq libraries
685 are generated from three biological replicates for Input (RNA-Seq) and m6A-
686 immunoprecipitated mRNA. Libraries are sequenced in a HiSeq 2000 with an average
687 coverage of 20 million reads per sample.
688

689 Reads are aligned against hg38 genome assembly with hisat 2.0.4 using the following
690 parameters: --no-unal --rna-strandness R. SAM files are sorted and converted to BAM
691 with samtools v1.7. Reads with QS < 10 are excluded, Normalized bigWig files are
692 generated from BAM files with bamCoverage from the deepTools suite v3.0.2 with the
693 following parameters: -bs 20 --normalizeUsing BPM --skipNAs. Reads that overlap with
694 the blacklisted regions from ENCODE project are excluded. Average bigWig files for the
695 biological replicates are generated using the bigwigCompare program from the
696 deepTools suite v3.0.2. m6A-enriched genes are obtained by calling significant peaks
697 form the BAM files with macs2 (v2.1.1) with a q-value < 1e-10 for each individual
698 biological replicate. A gene is considered to be enriched for m6A only if a peak was
699 called in all the replicates. Metagene and heatmap plots were generated with the
700 deepTools suite v3.0.2 and in-house scripts.
701
702 **PRO-Seq sequencing and analysis**
703 PRO-Seq libraries from 3 independent biological replicates were generated for Control
704 MEL624 cells, PCIF1-KO clone 1 and PCIF1-KO clone 2, using 1 million cells per
705 sample. Samples were spiked with 40,000 Drosophila S2 cells as a normalization spike-
706 in control. Samples were sequenced on the NextSeq using a High Output 75-cycle kit,
707 generating paired end 42 nt reads. Libraries were sequenced to an average read depth
708 of 50 million mappable reads per sample.
709

710 Paired-end reads were trimmed to 40 nt. To remove adapter sequence and low quality
711 3' ends we used cutadapt 1.14, discarding reads shorter than 20 nt (-m 20 -q 10), and
712 removing a single nucleotide from the 3' end of all trimmed reads to allow successful
713 alignment with Bowtie 1.2.2. Remaining read pairs were paired-end aligned to the
714 *Drosophila* dm3 genome index to determine spike-normalization ratios based on
715 uniquely mapped reads. Counts of pairs mapping uniquely to spike-in RNAs (drosophila
716 genome) were determined for each sample. In this case, the samples displayed highly
717 comparable recovery of spike-in reads, thus only depth normalization was used for each
718 bedGraph.
719
720 Reads mapped to dm3 were excluded from further analysis, and unmapped pairs were
721 aligned to the hg38 genome assembly. Identical parameters were utilized in each
722 alignment described above: up to 2 mismatches, maximum fragment length of 1000 nt,
723 and uniquely mappable, and unmappable pairs routed to separate output files (-m1, -v2,
724 -X1000, --un). Pairs mapping uniquely to hg38, representing biotin-labeled RNAs were
725 separated, and strand-specific counts of the 3'-end mapping positions determined at
726 single nucleotide resolution, genome-wide, and expressed in bedGraph format with
727 “plus” and “minus” strand labels, as appropriate. Combined bedGraphs were generated
728 after deduplication by summing counts per nucleotide of all 3 replicates for each
729 condition.
730

731 Read counts were calculated per gene (from transcription start site to transcription end
732 site), in a strand-specific manner, based on default annotations (ensembl hg38), using
733 featureCounts. Differentially expressed genes were identified using DESeq2 v1.18.1
734 under R 3.3.1. PRO-Seq size factors were determined based on DESeq2 (for Control:
735 0.9690449, 0.8752877, 0.9008983; PCIF1-KO1: 1.1669854, 0.9802904, 1.3105898;
736 PCIF1-KO2: 0.9866223, 1.0047620, 0.9516695). At an adjusted p-value threshold of
737 <0.01, 731 affected genes in KO clone 1 and 1406 in KO clone 2 were identified as
738 differentially expressed upon PCIF1-KO in MEL624 cells. After overlapping both lists
739 there are 506 genes that pass the padj < 0.01 threshold, from which 320 are
740 upregulated in both KO clone 1 and clone 2 (Table S4), 182 are downregulated in both
741 clones (Table S5) and 4 are downregulated in KO1 and upregulated in KO2. UCSC
742 Genome Browser tracks were generated from the combined replicates per condition,
743 normalized as in the differential expression analysis.
744
745 **RNA-Seq analysis**
746 Read counts for the RNAseq inputs from the m6A mapping experiment are calculated
747 from BAM files with featureCounts from the Rsubread package v1.22.3 in an R 3.3.3
748 environment. The read count table is analyzed with edgeR v3.12.1 and log2 TPM
749 measurements are generated. After calculating normalization factors and estimating
750 dispersion, DEG genes between KOs and Control cells were calculated using glm
751 modeling with a FDR < 1e-5. A final list of DEG shared between PCIF1 KO1 and PCIF1
752 KO2 is generated using in-house scripts, which gives a total of 236 upregulated genes

753 (Table S2) and 305 downregulated genes (Table S3). Boxplots of average expression
754 are generated with R 3.3.3 and in-house scripts from the log2 TPM values calculated in
755 edgeR. Mann-Whitney tests to compare average expression levels between different
756 samples and hyper geometric test to calculate p-values for overlaps between datasets
757 in Venn diagrams are performed in R 3.3.3.
758
759 **Microscale Thermophoresis (MST)**
760 RNA oligos used in MST analysis correspond to the first 219 nt 5' end of bicistronic
761 mRNAs used in Figure 7F. The 219 nucleotide m7G-Am capped RNA oligos are
762 transcribed using a PCR generated DNA template using the bicistronic construct
763 plasmid (pFR_CrPV_xb). Am methylated RNA oligo is further in vitro methylated to
764 m6Am using recombinant PCIF1. To generate decapped RNA control, m7G-Am
765 methylated RNA is decapped using a decapping enzyme. The RNA constructs are
766 column purified using Zymo RNA Clean & Concentrator kit after each transcription, in
767 vitro methylation step and decapping reaction.
768
769 The full-length human recombinant N terminal 6xHis tagged EIF4E protein is
770 fluorescently labelled in PBST with 0.1% PEG8000 using His-Tag Labelling Kit RED-
771 Tris-NTA (2nd Generation) (Nanotemper MO-L018). The RNA oligos are denatured at
772 65°C for 3 minutes followed by 1 minute immediate ice incubation. Then 2-fold serial
773 dilutions of RNA are carried out in PBST with 0.1% PEG800 at room temperature using
774 LoBind microfuge tubes. Labelled protein is added at 25 nM dye and 100 nM protein

775 final concentration to each RNA dilution. After 5 minute room temperature incubation,
776 premium capillaries are loaded and MST is carried out with 100% LED power and 40%
777 laser (20 seconds ON and 5 seconds OFF) using NanoTemper Control 1.1.9 software.
778 The binding constants are calculated using MO.Affinity Analysis V2.3 software using 10
779 dilution points carried out in triplicate independent binding assays for each RNA oligo.

780 **Supplemental Information**

781

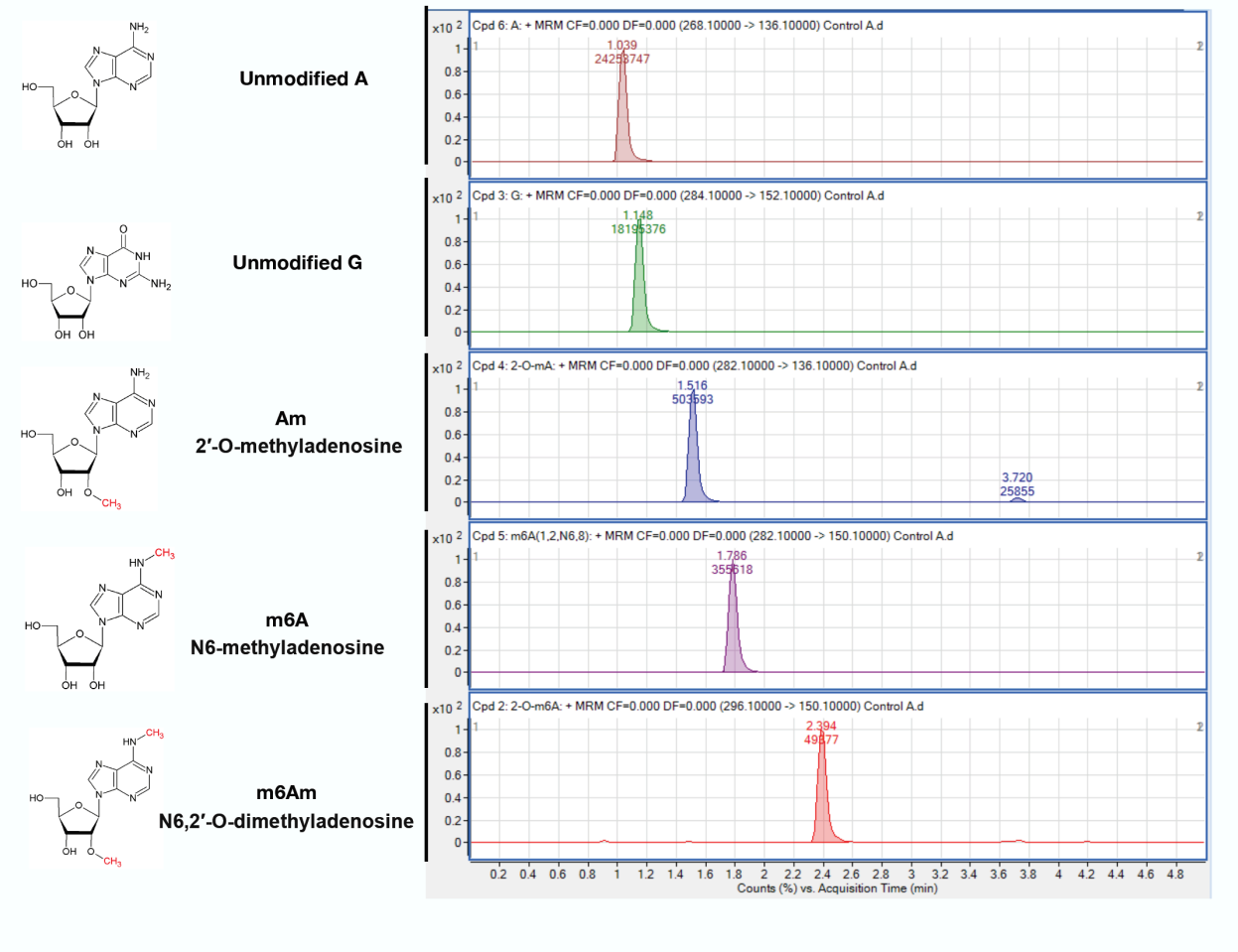

782

783

784 **Figure S1. Related to Figure 1.** Representative MS spectra of de-capped mRNA

785 from Mel624 human melanoma cell line.

786

Figure S2. Related to Figure 2. Alignment of protein sequences of zebrafish, mouse and human PCIF1 using ClustalW. The conserved methyltransferase motif is highlighted.

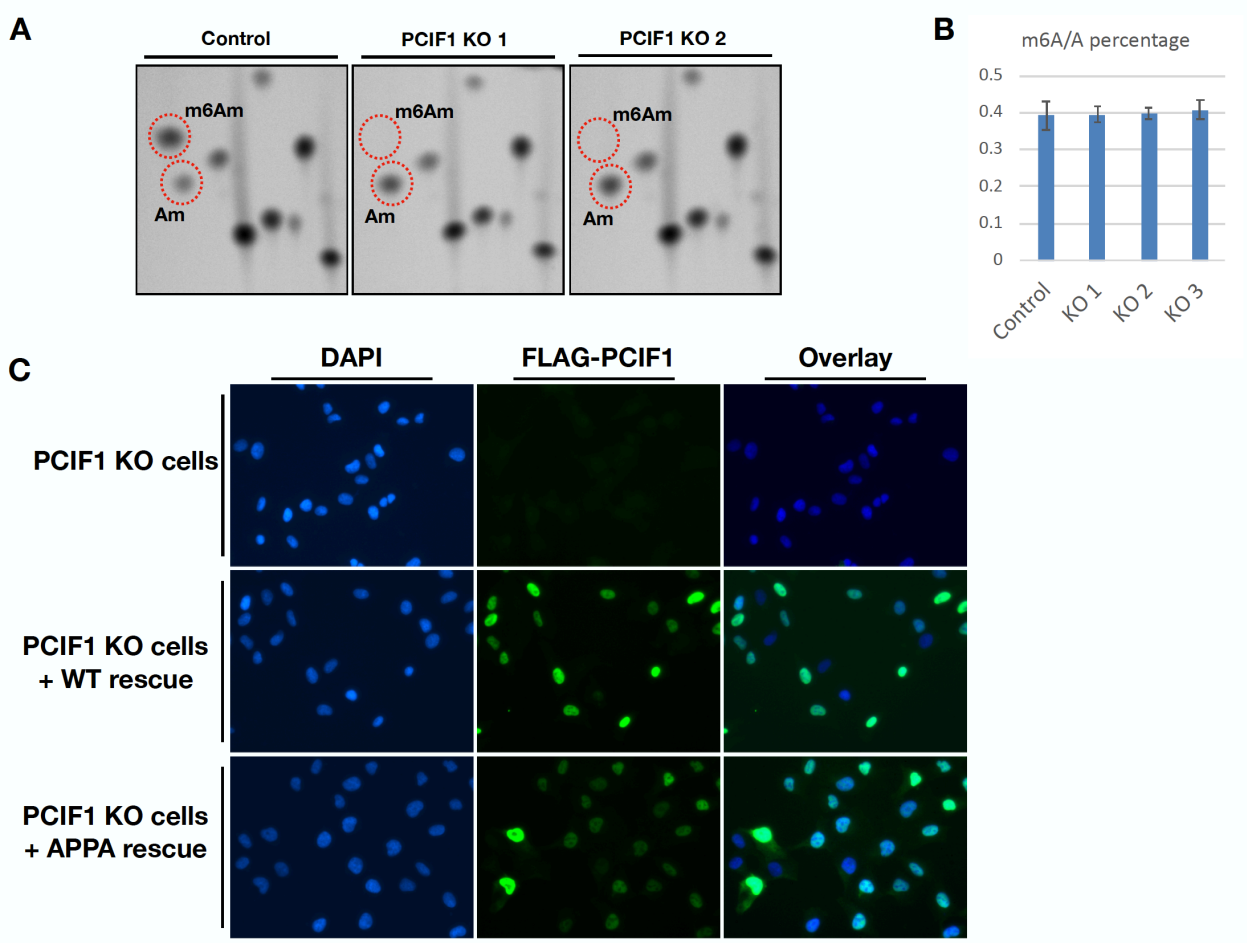

Figure S3. Related to Figure 2. PCIF1 is required for mRNA m6Am methylation in vivo.

3A. Thin-layer chromatography analysis of cap-adjacent nucleotides from mRNA isolated from control and two independent PCIF1 KO cell lines.
3B. LC-MS/MS m6A/A percentages of mRNAs from control and three independent PCIF1 KO cell lines
3C. Immunofluorescence images of PCIF1 KO and FLAG-PCIF1 rescue cell lines with anti-FLAG antibody.

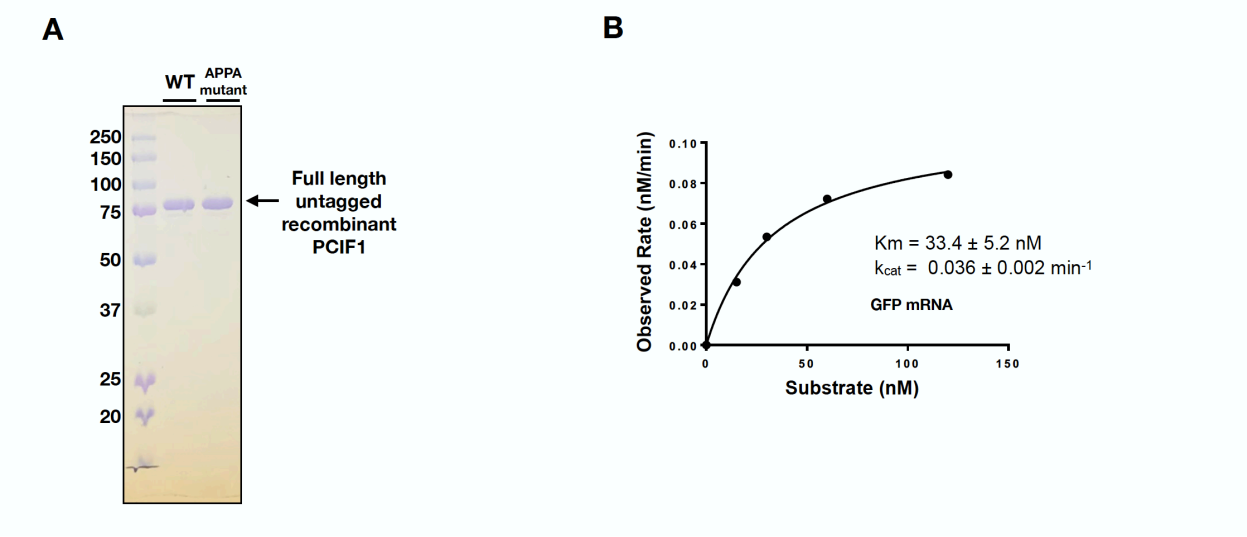

Figure S4. Related to Figure 3. *In vitro* enzyme kinetics with recombinant PCIF1

4A. GST tagged PCIF1 was expressed in bacteria and purified using Glutathine Sepharose beads and eluted using overnight thrombin cleavage. Around 3 μg of purified recombinant PCIF1 was run on PAGE gel and stained with Coomassie Blue.
4B. Michaelis–Menten kinetics of recombinant PCIF1 is determined using m7G-Am capped EGFP mRNA.

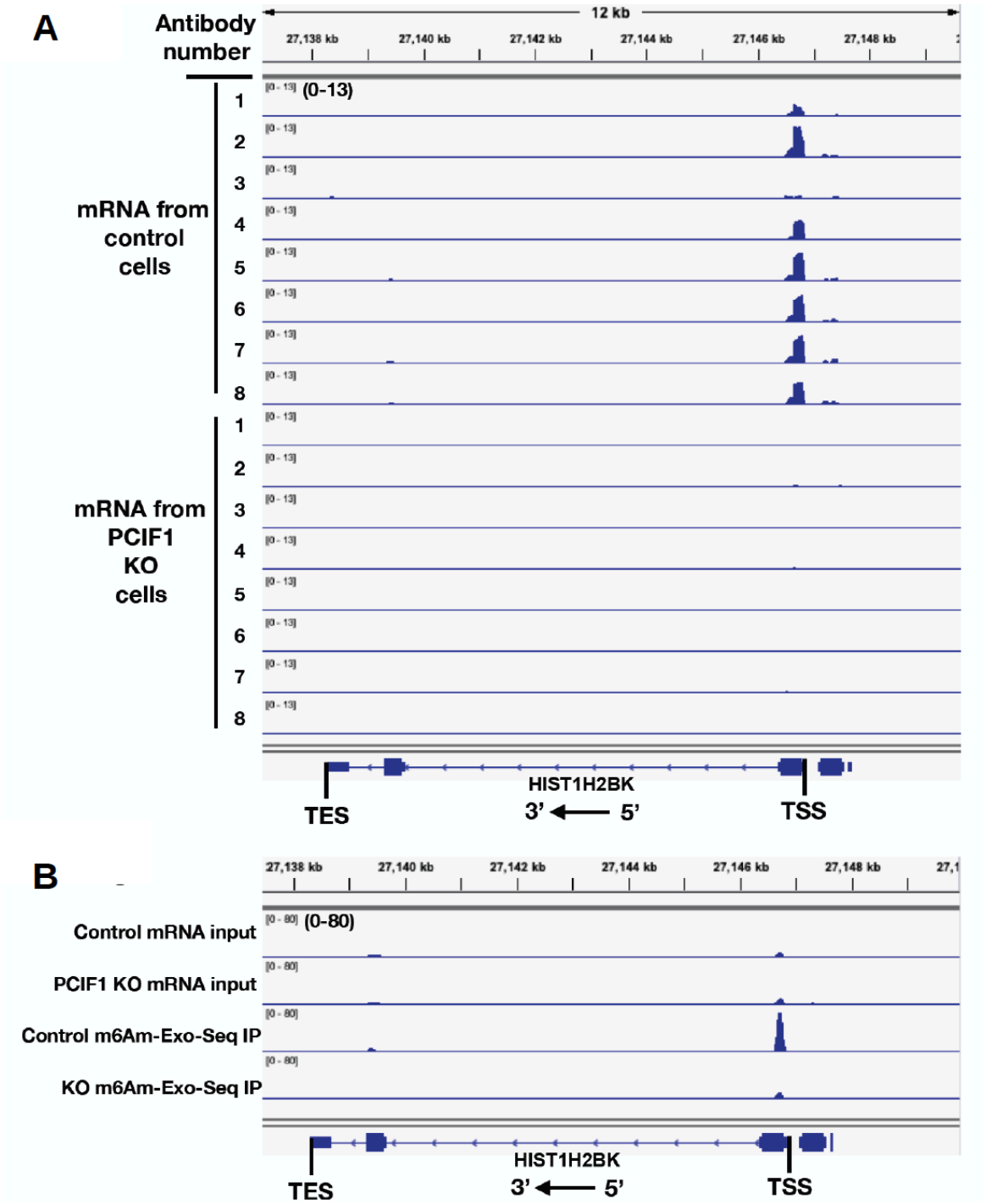

Figure S5. Related to Figure 5. Global mapping of m6Am through m6Am-Exo-Seq

5A. Genome browser view of m6Am-Exo-Seq fold change over input employing 8 different antibodies against m6A in control and PCIF1 KO cells.
5B. Genome browser view of reads per million in inputs and corresponding m6Am-Exo-Seq IPs from control and PCIF1 KO cells.

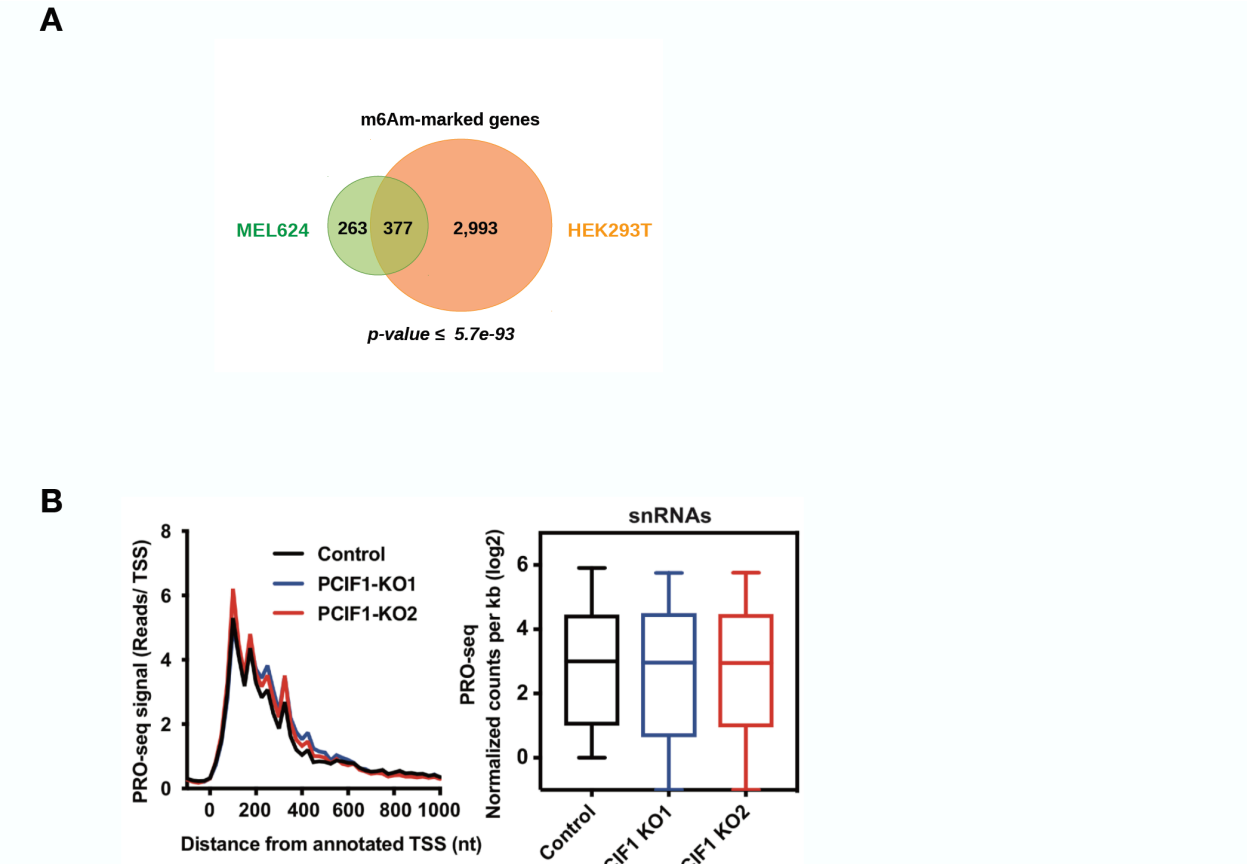

825
826
827 **Figure S6. Related to Figure 6. m6Am is cell type specific and does not**
828 **affect snRNA transcription**
829
830 6A. Venn diagram depicting overlap between 640 m6Am enriched genes in MEL624
831 and 3370 identified in HEK293T cells. P-values are calculated with a hypergeometric
832 test.
833 6B. PRO-Seq signal is shown at snRNA genes (N=667 snRNA genes expressed in
834 MEL624) in control and PCIF1 KO cells. Shown are a composite metagene distribution
835 (left) or boxplot of PRO-Seq signal within snRNA genes. Boxplots are shown as in 7D.
836 No significant differences were detected.
837

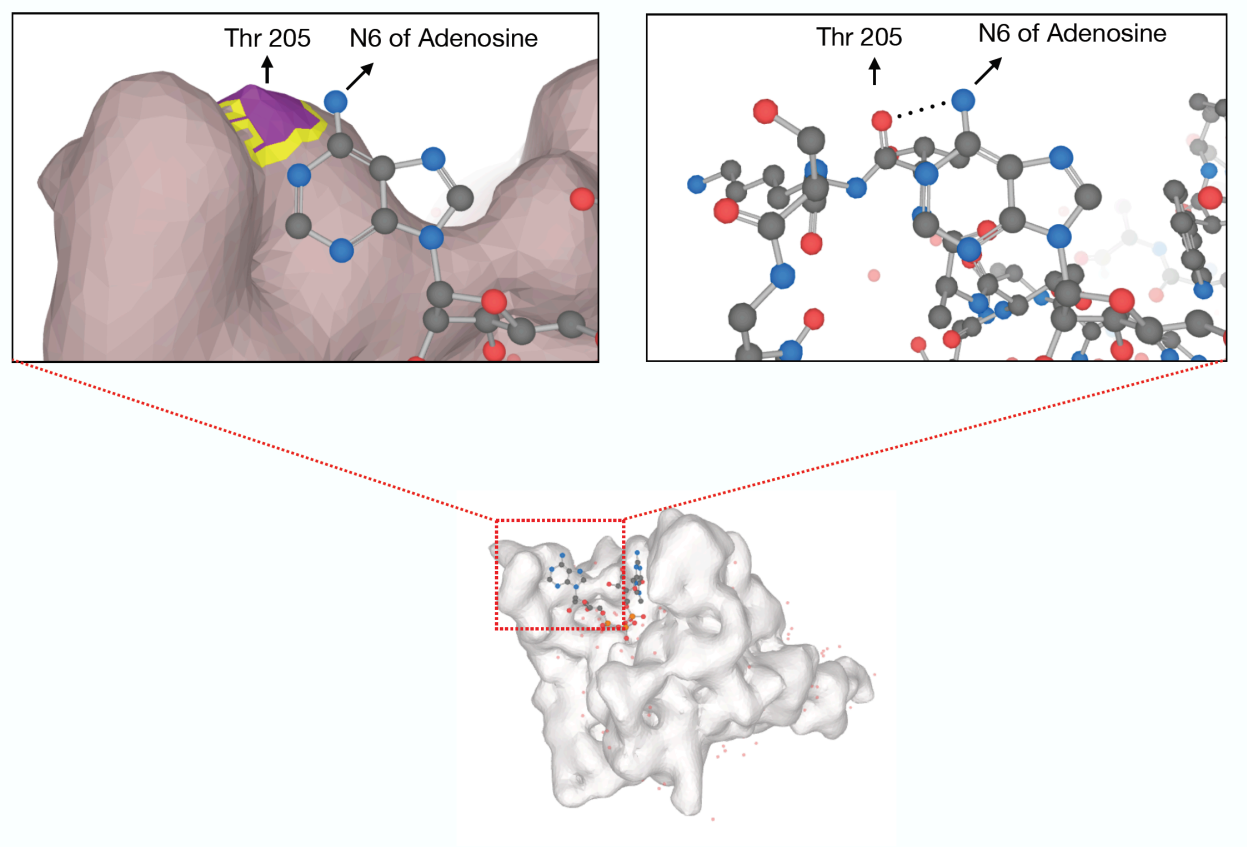

838
839
840 **Figure S7. Related to Figure 7.** N6 residue of cap adjacent adenosine of mRNA,
841 which gets m6A methylated by PCIF1, forms a hydrogen bond with threonine 205
842 residue of human eIF4E.
843

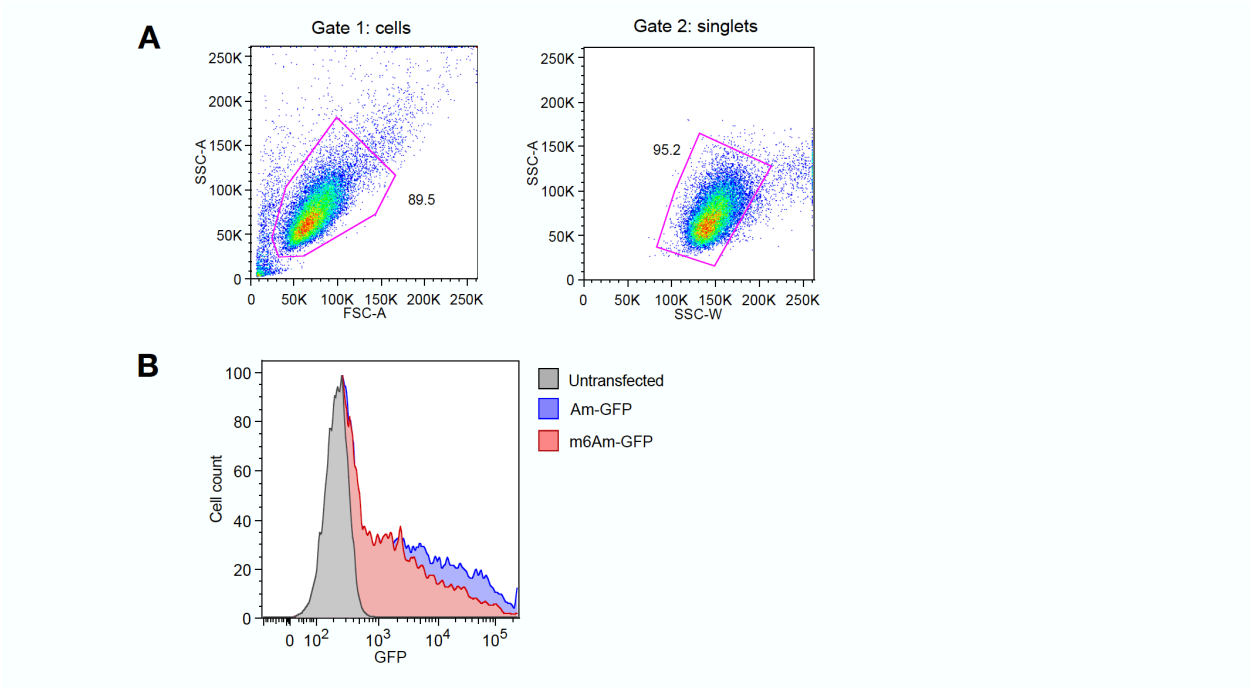

844
845
846 **Figure S8. Related to Figure 7. FACS analysis of Am or m6Am EGFP**
847 **transfected MEL624 cell lines.**
848
849 8A. Gating strategy for selecting singlet cells. Cells are gated based on FCS-A and
850 SSC-A (gate 1). Singlets are selected from gate 1 by gating SSC-W vs SSC-A. Cells
851 from gate 2 are used for all quantifications shown in Figure 7.
852 8B. Representative fluorescent profile of MEL624 cells transfected with Am- or m6Am-
853 EGFP mRNA. Untransfected cells are used as negative control.
854

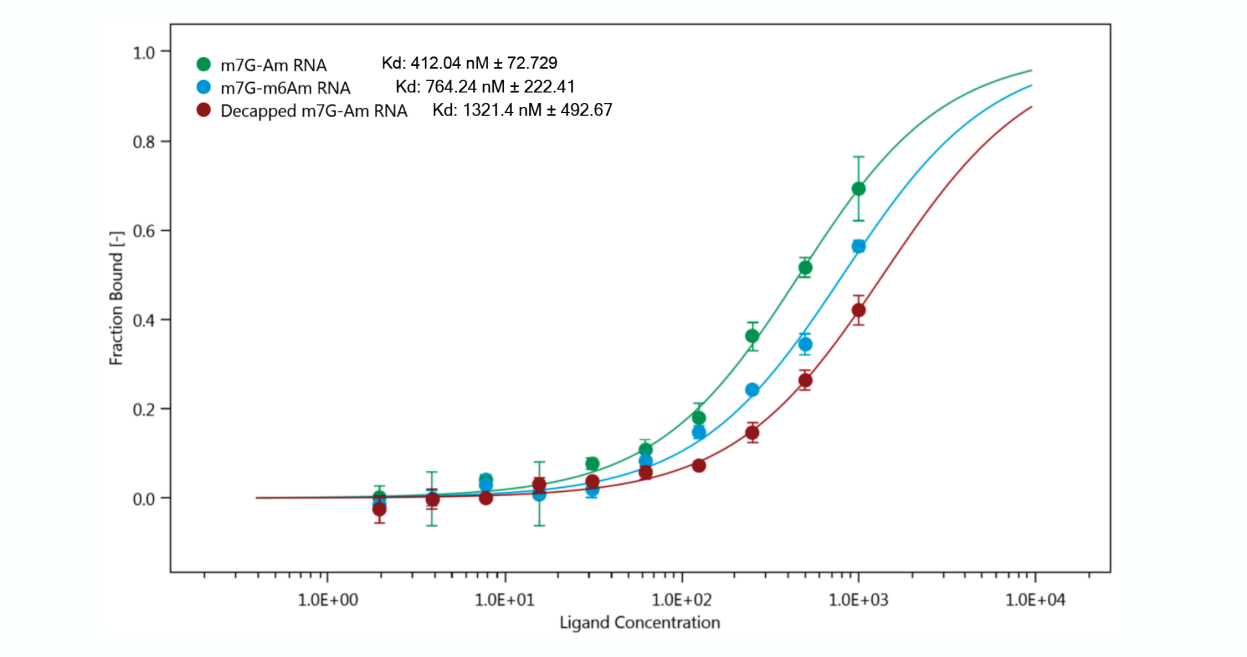

Figure S9. Related to Figure 7. Kd constants of fluorescently labelled N-terminal His tagged recombinant human eIF4E with 217 nt RNA oligos with either m7G-Am or m7G-m6Am 5' ends measured by microscale thermophoresis. De-capped m7G-Am RNA was used as a control. The 217 nucleotide RNA oligo sequence corresponds to the first 217 nt of bicistronic construct that was used in in vitro translation assays in Fig.7F. Three independent binding assays were performed with freshly labelled protein for each RNA oligo.

865 **Table S1. Related to Figure 5.** List of m6Am-marked genes.
866
867 **Table S2. Related to Figure 6.** List of Upregulated genes according to RNA-Seq
868
869 **Table S3. Related to Figure 6.** List of Downregulated genes according to RNA-Seq
870
871 **Table S4. Related to Figure 6.** List of Upregulated genes according to PRO-Seq
872
873 **Table S5. Related to Figure 6.** List of Downregulated genes according to PRO-
874 Seq
875